



HAL
open science

Asymptotic Performance Analysis of NOMA Uplink Networks Under Statistical QoS Delay Constraints

Mouktar Bello, Arsenia Chorti, Inbar Fijalkow, Wenjuan Yu, Leila Musavian

► **To cite this version:**

Mouktar Bello, Arsenia Chorti, Inbar Fijalkow, Wenjuan Yu, Leila Musavian. Asymptotic Performance Analysis of NOMA Uplink Networks Under Statistical QoS Delay Constraints. IEEE Open Journal of the Communications Society, 2020. hal-02972512

HAL Id: hal-02972512

<https://hal.science/hal-02972512>

Submitted on 20 Oct 2020

HAL is a multi-disciplinary open access archive for the deposit and dissemination of scientific research documents, whether they are published or not. The documents may come from teaching and research institutions in France or abroad, or from public or private research centers.

L'archive ouverte pluridisciplinaire **HAL**, est destinée au dépôt et à la diffusion de documents scientifiques de niveau recherche, publiés ou non, émanant des établissements d'enseignement et de recherche français ou étrangers, des laboratoires publics ou privés.

Asymptotic Performance Analysis of NOMA Uplink Networks Under Statistical QoS Delay Constraints

Mouktar Bello, *Student Member, IEEE*,

Arsenia Chorti, *Senior Member, IEEE*,

Inbar Fijalkow, *Senior Member, IEEE*, Wenjuan Yu, *Member, IEEE*, Leila Musavian *Senior Member, IEEE*

In this paper, we study the performance of an uplink non-orthogonal multiple access (NOMA) network under statistical quality of service (QoS) delay constraints, captured through each user's effective capacity (EC). We first propose novel closed-form expressions for the EC in a two-user NOMA network and show that in the high signal-to-noise ratio (SNR) region, the “strong” NOMA user, referred to as U_2 , has a limited EC, assuming the same delay constraint as the “weak” user, referred to as U_1 . We demonstrate that for the weak user U_1 , OMA and NOMA have comparable performance at low transmit SNRs, while NOMA outperforms OMA in terms of EC at high SNRs. On the other hand, for the strong user U_2 , NOMA achieves higher EC than OMA at small SNRs, while OMA becomes more beneficial at high SNRs. Furthermore, we show that at high transmit SNRs, irrespective of whether the application is delay tolerant, or not, the performance gains of NOMA over OMA for U_1 , and OMA over NOMA for U_2 remain unchanged. When the delay QoS of one user is fixed, the performance gap between NOMA and OMA in terms of total EC increases with decreasing statistical delay QoS constraints for the other user. Next, by introducing pairing, we show that NOMA with user-pairing outperforms OMA, in terms of total uplink EC. The best pairing strategies are given in the cases of four and six users NOMA, raising once again the importance of power allocation in the optimization of NOMA's performance.

Index Terms—Beyond 5G (B5G), effective capacity, low latency, non-orthogonal multiple access (NOMA), quality of service (QoS), user-pairing.

I. INTRODUCTION

Non-orthogonal multiple access (NOMA) schemes have attracted a lot of attention recently, allowing multiple users to be served simultaneously with enhanced spectral efficiency; it is known that the boundary of achievable rate pairs using NOMA is outside the capacity region achievable with orthogonal multiple access (OMA) techniques [1]–[5]. Superior achievable rates are attainable through the use of superposition coding at the transmitter and of successive interference cancellation (SIC) at the receiver [6]. The SIC receiver decodes multi-user signals with descending received signal power and subtracts the decoded signal(s) from the received superimposed signal, so as to improve the signal-to-interference ratio. The process is repeated until the signal of interest is decoded [7]. The interest in NOMA is linked to the multiple possibilities it offers, for example, in massive machine type communications (mMTC) systems where a large number of smart Internet of things (IoT) devices try to access the shared resources simultaneously.

In uplink NOMA networks, the strongest user's signal is decoded first (reverse order with respect to the downlink). However the use of SIC limits the promised performance gain brought by NOMA due to error propagation [8]–[10]. The authors in [11] introduce an iterative interference cancellation (IIC) detection scheme for uplink NOMA, and proposed a new detection scheme based on IIC, which is called advanced IIC

(AIIC). It is shown that the bit error rate performance of AIIC is much better than that of SIC.

Similarly, the combination of NOMA with other emerging techniques and technologies such as new modulation techniques, user pairing, resource allocation algorithms (power and channel), MIMO, etc., improves its performance [12]–[16]. The authors in [17] investigate the optimal power allocation in a NOMA system with two users, analyze user pairing in a NOMA system with four users and propose a closed-form globally optimal power allocation solution for a general NOMA downlink networks. In [18], an iterative gradient ascent-based power allocation method is proposed for downlink NOMA that achieves better performance compared to fixed and fractional power allocation strategies.

Furthermore, the power allocation strategy for energy efficient improvement in a downlink NOMA system is discussed in [19]. A novel power allocation algorithm based on particle swarm optimization is presented in [20]. To tackle the power allocation problem in downlink multi-carrier NOMA networks, a dynamic power allocation algorithm is proposed in [21], while a joint subchannel and power allocation is proposed based on the Dinkelbach algorithm in [22]. In the same framework, the joint power allocation and time switching control for energy efficiency optimization is investigated in [23], with the aim to optimize the energy efficiency of the system under maximum transmit power budget among others.

In [24], a novel prioritization-based buffer-aided relay selection scheme which is able to combine NOMA and OMA transmission in a relay network is proposed and an analytical expression for the average throughput of the proposed scheme is derived. In [25], dynamic and fixed power controls at users are discussed in the case of a cooperative uplink system with a buffer-aided NOMA and OMA transmission and an efficient buffer-aided hybrid NOMA/OMA based mode selection scheme is proposed. A hybrid OMA-NOMA scheme

M. Bello, A. Chorti and I. Fijalkow are with ETIS UMR8051, CY Cergy Paris University, ENSEA, CNRS, F-95000, Cergy, France, ({mouktar.bello, arsenia.chorti, inbar.fijalkow}@ensea.fr)

W. Yu is with the EEE Dep. of the Univ. of Lancaster (w.yu8@lancaster.ac.uk)

and L. Musavian is with the CSEE, Univ. of Essex (leila.musavian@essex.ac.uk). M. Bello is supported by the CY Tech Doctoral Training School, A. Chorti and I. Fijalkow are supported by the INEX project eNIGMA.

is presented in [26], in which NOMA is only employed if all users gain in terms of effective rates. Finally, NOMA offers a natural scenario for physical layer security as one user's signal is naturally degraded with respect to the other's [27] and constitutes the equivalent of a helping interferer [28].

Besides, in a number of emerging applications, delay constraints become increasingly important, e.g., ultra reliable low latency communication (URLLC) systems such as autonomous vehicles and enhanced reality. Furthermore, in future wireless networks, users are expected to necessitate flexible delay guarantees for achieving different service requirements. In order to satisfy diverse delay requirements, a simple and flexible delay quality of service (QoS) model is imperative to be applied and investigated. In this respect, the effective capacity (EC) theory can be employed [29]–[31]. The EC denotes the average maximum constant arrival rate which can be served by a given service process, while guaranteeing the required statistical delay provisioning [32].

The delay-constrained communications for a downlink NOMA network was studied in [33], where the EC theory was utilized. The present analysis on uplink complements [33] which focused on downlink transmissions. NOMA, as a more spectrum-efficient technique, is considered to be promising for supporting a massive number of devices in the uplink connections.

The present work extends our recent publication [34] in which novel closed form expressions for the effective rate in a two user uplink NOMA network were presented. Our contributions in this works are articulated around six lemmas and four propositions; the main contributions of this paper are listed below:

- First, using the theory of order statistics, we derive closed-form expressions for the effective capacity of each user in a two-user uplink NOMA network; The expressions are validated through Monte-Carlo simulations.
- We then provide an asymptotic analysis of the individual and sum ECs for both OMA and NOMA, in the case of delay-constrained and delay-tolerant applications. A detailed comparison between NOMA and OMA is provided; through an extensive set of simulation results, we show that NOMA does not always perform better than OMA in the presence of delay constraints. For illustration purposes, we depict the regions of the transmit signal-to-noise ratio (SNR) where the earlier outperforms the latter for generic values of the system parameters.
- With respect to the strong NOMA user, we prove that, its EC reaches a plateau in the high SNRs, in contrast to OMA, a consequence of the fact that the strong user is interference limited.
- The impact of the delay QoS exponent and of the transmit SNR on the individual and sum ECs is investigated as well. Specifically, we show that, through an extensive set of simulation results, the individual ECs decrease as the delay constraints becomes more stringent, and consequently so does the sum EC.
- Moreover, we investigate the impact of the choice of the user-pairing strategy on the sum EC. The best pairing strategy that maximizes the sum EC is shown, numer-

TABLE I
Notation Used

Notation	Parameters
M	Total number of users
U_i	User i
P_i	Allocated transmission power to U_i
P_T	Total power
ρ	Transmit SNR
θ_i	Delay QoS constraint of U_i
$ h_i ^2$	Channel gain of U_i
z	Received superimposed signal at the base station
R_i	Achievable rate of U_i under NOMA
\tilde{R}_i	Achievable rate of U_i under OMA
T_f	Duration of each fading-block
B	System bandwidth
β_i	Normalized QoS exponent
E_c^i	Effective capacity of i -th user NOMA
V_N	Sum ECs under NOMA
V_O	Sum ECs under OMA

ically, to be the pairing of users with the maximum channel gains gaps, which is in agreement to previous results in systems without delay constraints [35].

The rest of the paper is organized as follows. In Section II, we introduce the system model and define the notion of EC in an uplink NOMA system under delay QoS constraints. In Section III, an asymptotic analysis of the EC is provided for a two-user system. In Section IV, the EC of multiple pairs is studied to investigate the impact of pairing. Simulation results are given in Section V, followed by conclusions in Section VI.

II. EFFECTIVE CAPACITY IN UPLINK NOMA

The notation used throughout the rest of the paper is given in Table I for convenience.

A. General Case: M -User NOMA

Assume a M -user NOMA uplink network with users U_1, U_2, \dots, U_M in Rayleigh block-fading propagation channels [36], with respective channel gains during a transmission block denoted by $|h_i|^2, i = 1, \dots, M$, that without loss of generality are ordered as $|h_1|^2 < \dots < |h_M|^2$. The users transmit corresponding unit power symbols s_1, \dots, s_M respectively, with $\mathbb{E}[|s_i|^2] = 1, i = 1, \dots, M$ with a total transmit power constraint $P_T = \sum_{i=1}^M P_i = 1$. We note in passing that the total power constraint does not capture the individual user's budgets, but rather regulatory requirements imposing that the transmit power in any given resource block cannot exceed a maximum value [37]. The received superimposed signal can be expressed as [38]:

$$z = \sum_{i=1}^M \sqrt{P_i} h_i s_i + w, \quad (1)$$

where w denotes a zero mean circularly symmetric complex Gaussian random variable with variance σ^2 , i.e., $w \sim \mathcal{CN}(0, \sigma^2)$.

The receiver first decodes the symbols of the strongest user treating the transmission of the weaker users as interference. After decoding it, the receiver suppresses it from z and decodes the signal of the second strongest user, and so on until the decoding of the weakest user's signal. Following the SIC principle and denoting the transmit SNR $\rho = \frac{1}{\sigma^2}$, the achievable rate, in b/s/Hz, for user $U_i, i = 1, \dots, M$, assuming no error propagation, is expressed as [39]:

$$R_i = \log_2 \left(1 + \frac{\rho P_i |h_i|^2}{1 + \rho \sum_{l=1}^{i-1} P_l |h_l|^2} \right). \quad (2)$$

Notice that in the present work we don't consider the impact of path loss, but it could be easily taken into account by inserting a multiplicative coefficient on the user received SNR or SINR, accounting for the loss in received power due to distance. For the sake of simplicity, we do not account for this effect in the present, as common in related published work [1], [2], [33], [38].

Next, let θ_i be the statistical delay exponent of the i -th user, i.e., θ_i captures how strict the delay constraint of the user i is, and assume that the service process satisfies the Gärtner-Ellis theorem [30]. A slower decay rate can be represented by a smaller θ_i , which indicates that the system is more delay tolerant, while a larger θ_i corresponds to a system with more stringent QoS requirements. Applying the EC theory in an uplink NOMA with M users, the i -th user's EC over a block-fading channel is defined as:

$$E_c^i = -\frac{1}{\theta_i T_f B} \ln \left(\mathbb{E} \left[e^{-\theta_i T_f B R_i} \right] \right) \quad (\text{in b/s/Hz}), \quad (3)$$

where T_f is the duration of each fading-block, B is the system bandwidth and $\mathbb{E}[\cdot]$ denotes expectation over the channel gains. By inserting R_i into (3), we obtain the following expression for the EC of the i -th user

$$E_c^i = \frac{1}{\beta_i} \log_2 \left(\mathbb{E} \left[\left(1 + \frac{\rho P_i |h_i|^2}{1 + \rho \sum_{l=1}^{i-1} P_l |h_l|^2} \right)^{\beta_i} \right] \right) \quad (4)$$

where $\beta_i = -\frac{\theta_i T_f B}{\ln 2}$, $i = 1, \dots, M$, is the normalized (negative) QoS exponent. Developing (4), we have that:

$$E_c^i = \frac{1}{\beta_i} \log_2 \left(\int_0^\infty \int_{x_1}^\infty \int_{x_2}^\infty \dots \int_{x_{i-1}}^\infty \left(1 + \frac{\rho P_i x_i}{1 + \sum_{l=1}^{i-1} \rho P_l x_l} \right)^{\beta_i} f_{X(1), X(2), \dots, X(i)}(x_1, x_2, \dots, x_i) dx_i dx_{i-1} \dots dx_1 \right), \quad (5)$$

where $f_{X(1), X(2), \dots, X(i)}(x_1, x_2, \dots, x_i)$ is the joint distribution of $x_i = |h_i|^2, i = 1, \dots, M$.

To evaluate the joint distribution of the channel gains, we make use of the theory of order statistics [40]. The probability density function (PDF) of the i -th ordered random variable in a population of M is given by:

$$f_{X(i)}(x) = \psi_i f(x) (1 - F(x))^{M-i} F(x)^{i-1}, \quad (6)$$

where $\psi_i = \frac{1}{B(i, M-i+1)}$, and, $B(a, b)$ is the beta function $B(a, b) = \frac{\Gamma(a)\Gamma(b)}{\Gamma(a+b)}$, with $\Gamma(a) = (a-1)!$. Assuming a Rayleigh wireless environment, the channel gains, denoted

by $x_i = |h_i|^2$, are exponentially distributed with PDF and cumulative density function (CDF) respectively given by $f(x) = e^{-x}$, and $F(x) = 1 - e^{-x}$.

The joint distribution of M order statistics is given by [40]:

$$f_{X(1)\dots X(M)}(x_1, x_2, \dots, x_M) = M! f_{X(1)}(x_1) \dots f_{X(M)}(x_M), \quad (7)$$

where $x_1 \leq x_2 \leq \dots \leq x_M$, while for any two order statistics, we have that:

$$f_{X(l), X(k)}(x_l, x_k) = \frac{M!}{(l-1)!(k-l-1)!(M-k)!} \times (1 - F(x))^{l-1} f(x) (F(x) - F(y))^{k-l-1} f(y) (F(y))^{M-k}. \quad (8)$$

Closed-form expressions for multi-users uplink NOMA can be obtained by inserting (7) into (5), but considering the complexity of the analytical development of these integrals, we will just consider in this study, the simple case of two users. Furthermore, there is also a question of practical limitation. In fact, the execution of several SICs in series at the base station can lead to additional processing delay; thus, an increase in terms of latency, especially for the last decoded user. Moreover, if we have imperfect SIC, additional errors due to error propagation can lead to decoding failure for weaker users, as they are the last to be decoded [41]. Due to the above reasons, in the following we focus on deriving closed-form expressions only for the two-user case.

B. Case of Two-User NOMA Uplink Network ($M=2$)

Using (6), we obtain

$$f_{X(1)}(x_1) = 2e^{-2x_1}. \quad (9)$$

Furthermore, by setting $M = 2, l = 1$ and $k = 2$ in (8), we get:

$$f_{X(1), X(2)}(x_1, x_2) = 2f(x_1)f(x_2) = 2e^{-x_1}e^{-x_2}. \quad (10)$$

As a result, the EC of U_1 , denoted by E_c^1 , is expressed as

$$\begin{aligned} E_c^1 &= \frac{1}{\beta_1} \log_2 \left(\mathbb{E}[(1 + \rho P_1 x_1)^{\beta_1}] \right) \\ &= \frac{1}{\beta_1} \log_2 \left(\int_0^\infty (1 + \rho P_1 x_1)^{\beta_1} f_{X(1)}(x_1) dx_1 \right) \\ &= \frac{1}{\beta_1} \log_2 \left(\frac{2}{P_1 \rho} \times U \left(1, 2 + \beta_1, \frac{2}{\rho P_1} \right) \right), \quad (11) \end{aligned}$$

where $U(\cdot, \cdot, \cdot)$ denotes the confluent hypergeometric function [33].

On the other hand, the EC of U_2 is evaluated as

$$\begin{aligned}
 E_c^2 &= \frac{1}{\beta_2} \log_2 \left(\mathbb{E} \left[\left(1 + \frac{\rho P_2 x_2}{1 + \rho P_1 x_1} \right)^{\beta_2} \right] \right) \\
 &= \frac{1}{\beta_2} \log_2 \left(\int_0^\infty \int_{x_1}^\infty \left(1 + \frac{\rho P_2 x_2}{1 + \rho P_1 x_1} \right)^{\beta_2} f_{x(1), x(2)}(x_1, x_2) dx_2 dx_1 \right) \\
 &= \frac{1}{\beta_2} \log_2 \left(2P_2^{1-\beta_2} (\rho P_2)^{\beta_2} e^{\frac{1}{\rho P_2}} e^{-\frac{(P_1 - P_2)}{\rho P_2}} \right) \\
 &+ \frac{1}{\beta_2} \log_2 \left(\sum_{j=0}^{-\beta_2} \binom{-\beta_2}{j} (\rho P_1)^j \times \sum_{k=0}^\infty \frac{(-1)^k (P_2 - P_1)^k}{k! (1 + j + k)} \right) \\
 &\times \left[\Gamma \left(2 + \beta_2 + j + k, \frac{1}{\rho P_2} \right) - (\rho P_2)^{-1-j-k} \Gamma \left(1 + \beta_2, \frac{1}{\rho P_2} \right) \right] \quad (12)
 \end{aligned}$$

with $\Gamma(\cdot, \cdot)$ denoting the incomplete Gamma function [33].

Proof: The proof is provided in Appendix I. ■

The closed-form expression of the sum EC in the case of a two-user NOMA uplink network can be easily obtained by summing up the individual ECs.

C. Case of a Two-User OMA Network

Similarly, using time division multiple access (TDMA), the achievable data rate of the i -th user in a two-user OMA network, denoted by $\tilde{R}_i, i = 1, 2$, is given by

$$\tilde{R}_i = \frac{1}{2} \log_2 \left(1 + 2\rho P_i |h_i|^2 \right), i = 1, 2. \quad (13)$$

Note that $\frac{1}{2}$ is due to the equal allocation of resources to both users. Furthermore, it is important to note that the power of each OMA user is double that of NOMA, for the sake of fairness [33]. The corresponding ECs of both users in an OMA network are denoted by \tilde{E}_c^i :

$$\tilde{E}_c^i = \frac{1}{\beta_i} \log_2 \left(\mathbb{E} \left[\left(1 + 2\rho P_i |h_i|^2 \right)^{\frac{\beta_i}{2}} \right] \right). \quad (14)$$

A general expression of the ECs of M TDMA OMA users is given in [33]; applying this to a two-user network we can be easily obtain:

$$\tilde{E}_c^1 = \frac{1}{\beta_1} \log_2 \left(\frac{1}{\rho P_1} \times U \left(1, 2 + \frac{\beta_1}{2}, \frac{1}{\rho P_1} \right) \right), \quad (15)$$

$$\tilde{E}_c^2 = \frac{1}{\beta_2} \log_2 \left(\frac{1}{\rho P_2} \sum_{k=0}^1 \binom{1}{k} (-1)^k \times U \left(1, 2 + \frac{\beta_2}{2}, \frac{1+k}{2\rho P_2} \right) \right). \quad (16)$$

The difference in these expressions is due to the different PDFs of ordered channel gains.

III. ASYMPTOTIC ANALYSIS

In this Section, an asymptotic analysis with respect to the transmit SNR ρ is presented. This analysis consists in describing the limiting behavior of individual and total ECs, and how they evolve with the transmit SNR ρ . Our results are summarized in the following Propositions and Lemmas.

A. Case 1: Delay-Constrained Users

Proposition 1:

- 1) At low transmit SNR, $\rho \rightarrow 0$, $E_c^1, \tilde{E}_c^1, E_c^2$ and \tilde{E}_c^2 start at zero and then increase at the same rate for any user.
- 2) At high values of the transmit SNR, $\rho \gg 1$, E_c^1 increases faster than \tilde{E}_c^1 and NOMA becomes more advantageous than OMA, for U_1 . While for U_2 , \tilde{E}_c^2 increases faster than E_c^2 , although NOMA is outperforming OMA.
- 3) At very high values of the transmit SNR, $\rho \rightarrow \infty$, the performance gain of NOMA over OMA increases at gradually reducing rate, for U_1 . Albeit, for U_2 , E_c^2 reaches an upper limit, allowing OMA to outperform NOMA after some SNR value (which depends on the system parameters).

Proposition 1 is the synthesis of **Lemmas 1, 2 and 3**, discussed in detail next.

Lemma 1: In the low and high SNR regimes, respectively, the following conclusions hold:

- 1) When $\rho \rightarrow 0$, then, $E_c^1 \rightarrow 0, E_c^2 \rightarrow 0, \tilde{E}_c^1 \rightarrow 0, \tilde{E}_c^2 \rightarrow 0, E_c^1 - \tilde{E}_c^1 \rightarrow 0, E_c^2 - \tilde{E}_c^2 \rightarrow 0$;
- 2) When $\rho \rightarrow +\infty$, then $E_c^1 \rightarrow +\infty, E_c^2 \rightarrow \frac{1}{\beta_2} \log_2 \left(\mathbb{E} \left[\left(1 + \frac{P_2 |h_2|^2}{P_1 |h_1|^2} \right)^{\beta_2} \right] \right), \tilde{E}_c^1 \rightarrow +\infty, \tilde{E}_c^2 \rightarrow +\infty, E_c^1 - \tilde{E}_c^1 \rightarrow +\infty, E_c^2 - \tilde{E}_c^2 \rightarrow -\infty$.

Proof: The proof is provided in Appendix II. ■

To further analyze the impact of ρ on the individual EC, the partial derivatives with the respect of ρ are investigated [33].

Lemma 2: For the EC of the U_1 , in a two-user uplink network the following hold:

- 1) $\frac{\partial E_c^1}{\partial \rho} \geq 0$ and $\frac{\partial \tilde{E}_c^1}{\partial \rho} \geq 0, \forall \rho$;
- 2) When $\rho \rightarrow 0$, then $\lim_{\rho \rightarrow 0} \left(\frac{\partial (E_c^1 - \tilde{E}_c^1)}{\partial \rho} \right) = 0$;
- 3) When $\rho \gg 1$, then $\frac{\partial (E_c^1 - \tilde{E}_c^1)}{\partial \rho} \approx \frac{1}{2\rho \ln 2} \geq 0$ and it approaches 0 when $\rho \rightarrow \infty$.

Proof: The proof is provided in Appendix III. ■

Lemma 3: For the EC of the U_2 , in a two-user uplink network the following hold:

- 1) $\frac{\partial E_c^2}{\partial \rho} \geq 0$ and $\frac{\partial \tilde{E}_c^2}{\partial \rho} \geq 0, \forall \rho$;
- 2) When $\rho \rightarrow 0$, then $\lim_{\rho \rightarrow 0} \left(\frac{\partial (E_c^2 - \tilde{E}_c^2)}{\partial \rho} \right) = 0$
- 3) When $\rho \gg 1$, then $\frac{\partial (E_c^2 - \tilde{E}_c^2)}{\partial \rho} \approx -\frac{1}{2 \ln 2} \frac{1}{\rho} < 0$ and it approaches 0 when $\rho \rightarrow \infty$.

Proof: The proof is provided in Appendix IV. ■

Finally, we investigate the sum ECs when using OMA and NOMA, denoted by V_N and V_O , respectively, i.e.,

$$V_N = E_c^1 + E_c^2, \quad (17)$$

$$V_O = \tilde{E}_c^1 + \tilde{E}_c^2. \quad (18)$$

Proposition 2:

- 1) At low transmit SNR ρ , V_N and V_O increase at a constant rate that depends on the average of the channel power gains and the allocated power coefficients.
- 2) When $\rho \gg 1$, V_N and V_O tend to ∞ , and reach a plateau when the transmit SNR $\rho \rightarrow \infty$.

Proposition 2 is the consequence of the **Lemma 4**.

Lemma 4: For the sum EC with NOMA, denoted by V_N , and with OMA, denoted by V_O , in a two-user uplink network, the following hold:

- 1) $\frac{\partial V_N}{\partial \rho} \geq 0$ and $\frac{\partial V_O}{\partial \rho} \geq 0, \forall \rho$;
- 2) When $\rho \rightarrow 0, V_N \rightarrow 0, \lim_{\rho \rightarrow 0}(\frac{\partial V_N}{\partial \rho}) = \frac{P_1}{\ln 2} \mathbb{E}[|h_1|^2] + \frac{P_2}{\ln 2} \mathbb{E}[|h_2|^2] \geq 0$, and $V_O \rightarrow 0, \lim_{\rho \rightarrow 0}(\frac{\partial V_O}{\partial \rho}) = \frac{P_1}{\ln 2} \mathbb{E}[|h_1|^2] + \frac{P_2}{\ln 2} \mathbb{E}[|h_2|^2] \geq 0$;
- 3) When $\rho \gg 1, V_N \rightarrow \infty, \lim_{\rho \rightarrow \infty}(\frac{\partial V_N}{\partial \rho}) = 0$, and $V_O \rightarrow \infty, \lim_{\rho \rightarrow \infty}(\frac{\partial V_O}{\partial \rho}) = 0$.

Proof: The proof is provided in Appendix V. ■

B. Case 2: Delay-Tolerant Applications

A case of particular interest is presented when the users' applications are delay tolerant, i.e., when the delay exponent becomes negligible. In this case, investigation of the ECs of the two-user, uplink NOMA and OMA networks, is performed without delay constraints. The impact of the transmit SNR ρ in this case is also investigated.

Proposition 3:

- 1) For both OMA and NOMA, when there is no delay constraint ($\theta = 0$), the individual ECs of both users are equal to their ergodic capacities.
- 2) At high transmit SNRs, irrespective of whether there's a tolerance for delay or not, the conclusions on the performance gain of NOMA over OMA for U_1 , and OMA over NOMA for U_2 remain the same.

Proposition 3 is the consequence of the **Lemma 5**.

Lemma 5: Considering the EC for the weaker user with $\theta_1 \rightarrow 0$, in NOMA and OMA, the following hold:

- a) When $\theta_1 \rightarrow 0, \lim_{\theta_1 \rightarrow 0} E_c^1 = \mathbb{E}[R_1], \lim_{\theta_1 \rightarrow 0} \tilde{E}_c^1 = \mathbb{E}[\tilde{R}_1], \lim_{\theta_1 \rightarrow 0} (E_c^1 - \tilde{E}_c^1) = \mathbb{E}[R_1] - \mathbb{E}[\tilde{R}_1]$,
- b) When $\theta_1 \rightarrow 0, \rho \rightarrow \infty, \lim_{\rho \rightarrow \infty} E_c^1 = \infty, \lim_{\rho \rightarrow \infty} \tilde{E}_c^1 = \infty, \lim_{\rho \rightarrow \infty} (E_c^1 - \tilde{E}_c^1) = \infty$.

Considering the EC for the stronger user with $\theta_2 \rightarrow 0$, in NOMA and OMA, we prove that:

- c) When $\theta_2 \rightarrow 0, \lim_{\theta_2 \rightarrow 0} E_c^2 = \mathbb{E}[R_2], \lim_{\theta_2 \rightarrow 0} \tilde{E}_c^2 = \mathbb{E}[\tilde{R}_2], \lim_{\theta_2 \rightarrow 0} (E_c^2 - \tilde{E}_c^2) = \mathbb{E}[R_2] - \mathbb{E}[\tilde{R}_2]$,
- d) When $\theta_2 \rightarrow 0, \rho \rightarrow \infty, \lim_{\rho \rightarrow \infty} E_c^2 = \mathbb{E}\left[\log_2\left(1 + \frac{P_2|h_2|^2}{P_1|h_1|^2}\right)\right], \lim_{\rho \rightarrow \infty} \tilde{E}_c^2 = \infty, \lim_{\rho \rightarrow \infty} (E_c^2 - \tilde{E}_c^2) = -\infty$.

Proof: The proof is provided in Appendix VI. ■

IV. EFFECTIVE CAPACITY OF MULTIPLE NOMA PAIRS

The M NOMA users scenario assumes that the resource block is shared among M users. For large values of M , stronger users are penalized due to high interference level from weaker users since they are decoded first. Pairing allows us

to mitigate interference from weaker users on stronger ones. A popular approach for alleviating this effect in an M user network, is to form $\frac{M}{2}$ groups with indices $i = 1, \dots, \frac{M}{2}$, where each group involves only 2 users. Inside each group, NOMA is implemented, while across different groups TDMA is applied.

The achievable data rate of the two users, U_1 and U_2 of the i^{th} group, where $|h_{1_i}|^2 \leq |h_{2_i}|^2$, can be formulated as follow:

$$R_{1_i} = \frac{2}{M} \log_2(1 + \rho P_{1_i} |h_{1_i}|^2), \quad (19)$$

$$R_{2_i} = \frac{2}{M} \log_2\left(1 + \frac{\rho P_{2_i} |h_{2_i}|^2}{1 + \rho P_{1_i} |h_{1_i}|^2}\right), \quad (20)$$

with $\frac{2}{M}$ the fraction of resources at the disposal of the two users inside a NOMA group.

On the other hand, if all users utilize TDMA, their achievable data rates are given as follows:

$$\tilde{R}_j = \frac{1}{M} \log_2(1 + 2P_j \rho |h_j|^2), j \in \{1_i, 2_i\}. \quad (21)$$

The factor $\frac{1}{M}$ is to indicate that each user has only one time slot to transmit.

By replacing (19) and (20) in (3), we get respectively the following ECs for U_1 and U_2 in the i^{th} group:

$$E_c^{1_i} = \frac{1}{\beta_{1_i}} \log_2\left(\mathbb{E}\left[\left(1 + \rho P_{1_i} |h_{1_i}|^2\right)^{\frac{2\beta_{1_i}}{M}}\right]\right), \quad (22)$$

$$E_c^{2_i} = \frac{1}{\beta_{2_i}} \log_2\left(\mathbb{E}\left[\left(1 + \frac{\rho P_{2_i} |h_{2_i}|^2}{1 + \rho P_{1_i} |h_{1_i}|^2}\right)^{\frac{2\beta_{2_i}}{M}}\right]\right). \quad (23)$$

On the other hand, replacing (21) in (3) we get the expressions for both users while using TDMA:

$$\tilde{E}_c^{1_i} = \frac{1}{\beta_{1_i}} \log_2\left(\mathbb{E}\left[\left(1 + 2\rho P_{1_i} |h_{1_i}|^2\right)^{\frac{\beta_{1_i}}{M}}\right]\right), \quad (24)$$

$$\tilde{E}_c^{2_i} = \frac{1}{\beta_{2_i}} \log_2\left(\mathbb{E}\left[\left(1 + 2\rho P_{2_i} |h_{2_i}|^2\right)^{\frac{\beta_{2_i}}{M}}\right]\right). \quad (25)$$

Next, we analyze the total sum EC of multiple NOMA pairs, denoted by E_c^{tot} , in comparison with the total sum EC for the M OMA users, \tilde{E}_c^{tot} defined as:

$$E_c^{tot} = \sum_{i=1}^{\frac{M}{2}} (E_c^{1_i} + E_c^{2_i}), \quad (26)$$

$$\tilde{E}_c^{tot} = \sum_{i=1}^{\frac{M}{2}} (\tilde{E}_c^{1_i} + \tilde{E}_c^{2_i}). \quad (27)$$

To investigate the performance of the user-pairing, the following Proposition and Lemma are provided.

Proposition 4:

- 1) NOMA user-pairing outperforms OMA at low transmit SNRs and this performance gain carries on at very high transmit SNRs, with the possibility to be improved by optimizing the power allocation.

Proposition 4 is the consequence of **Lemma 6**.

Lemma 6: Considering $E_c^{tot} - \widetilde{E}_c^{tot}$, we prove that:

- a) When $\rho \rightarrow 0$, $E_c^{tot} - \widetilde{E}_c^{tot} \rightarrow 0$, and $\lim_{\rho \rightarrow 0} \frac{\partial(E_c^{tot} - \widetilde{E}_c^{tot})}{\partial \rho} = 0$.
- b) When $\rho \rightarrow \infty$, $E_c^{tot} - \widetilde{E}_c^{tot} \rightarrow \text{constant}$, given in (28), and $\lim_{\rho \rightarrow \infty} \frac{\partial(E_c^{tot} - \widetilde{E}_c^{tot})}{\partial \rho} = 0$.

$$\lim_{\rho \rightarrow \infty} (E_c^{tot} - \widetilde{E}_c^{tot}) = \sum_{i=1}^{\frac{M}{2}} \left(\frac{1}{\beta_{1,i}} \log_2 \left(2^{-\frac{\beta_{1,i}}{M}} \mathbb{E} \left[(P_{1,i} |h_{1,i}|^2)^{\frac{\beta_{1,i}}{M}} \right] \right) \right) + \frac{1}{\beta_{2,i}} \log_2 \left(\frac{\mathbb{E} \left[\left(1 + \frac{P_{2,i} |h_{2,i}|^2}{P_{1,i} |h_{1,i}|^2} \right)^{\frac{2\beta_{2,i}}{M}} \right]}{\mathbb{E} \left[(2P_{2,i} |h_{2,i}|^2)^{\frac{\beta_{2,i}}{M}} \right]} \right) \right). \quad (28)$$

Proof: The proof is provided in Appendix VII. ■

From **Lemma 6**, we can conclude that $E_c^{tot} - \widetilde{E}_c^{tot}$ initially starts at 0, first increases at low transmit SNRs ρ , and finally approaches the *constant* value given in (28) that depends on the power allocation, at high transmit SNRs, i.e., this performance gain of NOMA with user-pairing over OMA can be optimized by finding the best pairing strategy.

V. NUMERICAL RESULTS

In this Section, the Propositions and Lemmas presented in previous sections are validated through Monte-Carlo simulations. We first consider a two-user uplink NOMA system, with the following parameters: normalized transmission power for both users, $P_1 = 0.2$, $P_2 = 0.8$, normalized delay exponent $\beta_1 = \beta_2 = -1$ for both users, unless otherwise stated. Fixed power allocation is used for the sake of simplicity.

Fig.1 provides validation of the proposed closed-form expressions of E_c^1 and E_c^2 respectively in (11) and (12). The analytical expressions of these individual ECs (—, —) and the corresponding Monte-Carlo simulations (—, —) are indistinguishable, showcasing the accuracy of the proposed closed-form expressions.

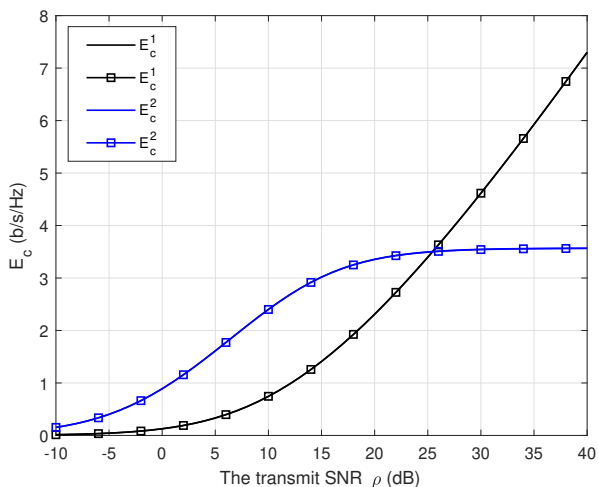


Fig. 1. Validation of the closed-form expressions in uplink two-user NOMA system.

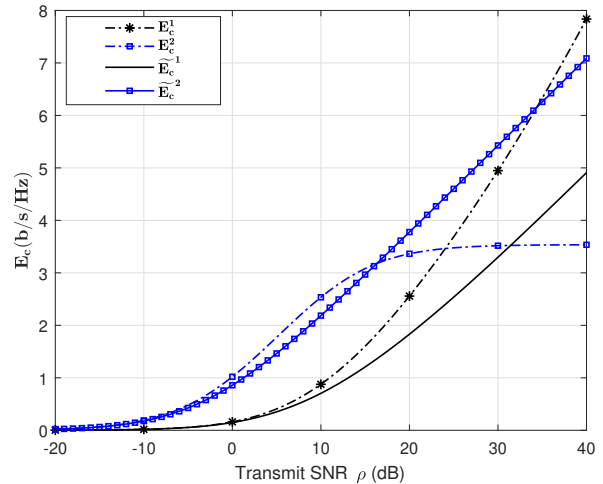


Fig. 2. E_c^1 , E_c^2 , and \widetilde{E}_c^1 , \widetilde{E}_c^2 , versus the transmit SNR ρ

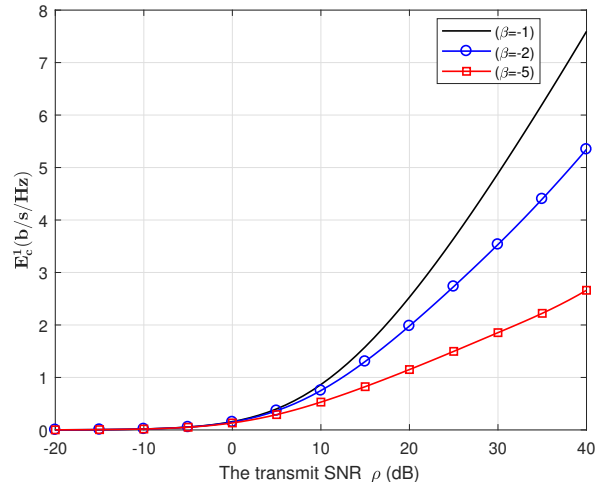


Fig. 3. E_c^1 versus the transmit SNR, for different delay requirements.

In Fig.2, the ECs of the two-user uplink NOMA and OMA networks are depicted versus the transmit SNR. We note that for U_1 , NOMA and OMA perform equally well at very low transmit SNRs, and NOMA is advantageous compared to OMA at high transmit SNRs. In contrast, for U_2 , NOMA is better at low SNRs and OMA is advantageous at high transmit SNRs. We notice also that the EC of U_2 reaches a plateau at high SNRs, validating **Lemma 1**. Moreover, we note that, at low transmit SNRs, E_c^2 is higher than E_c^1 , despite the interference that U_2 experiences; but with the transmit SNR increasing, E_c^1 increases without bound and therefore at some point surpasses E_c^2 which is capped to an upper value.

Fig.3 and Fig.4 show, respectively, the EC of U_1 and U_2 , versus the transmit SNR, for different values of the delay exponent. When the delay constraints become more stringent, i.e., β decreases (equivalently, θ increases), both E_c^1 and E_c^2 decrease.

In Fig. 5, the ECs of the strong and weak users are depicted

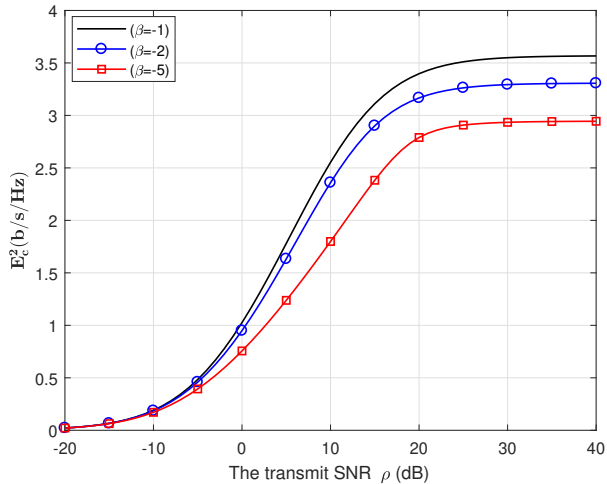


Fig. 4. E_c^2 versus the transmit SNR ρ for different delay requirements.

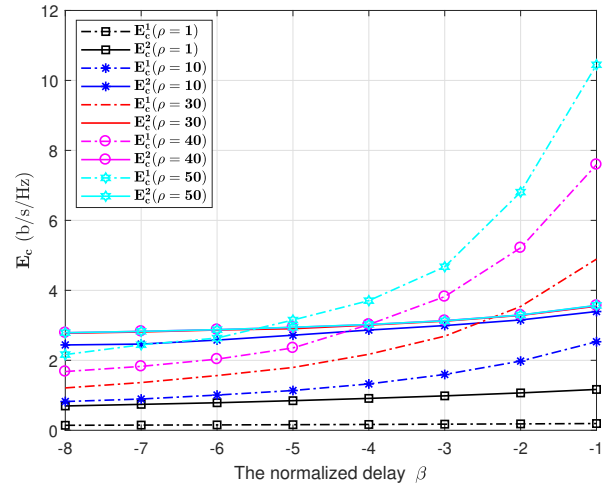


Fig. 6. E_c^1, E_c^2 versus normalized delay β , for different values of ρ .

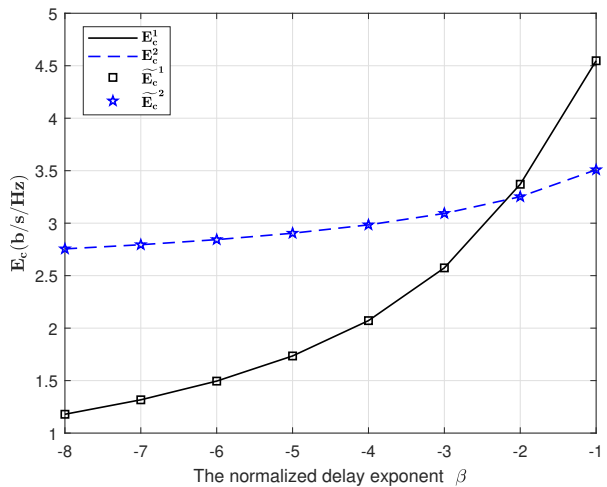


Fig. 5. E_c^1, E_c^2 , and \widetilde{E}_c^1 and \widetilde{E}_c^2 , versus the (negative) normalized delay exponent β at $\rho = 30$ dB.

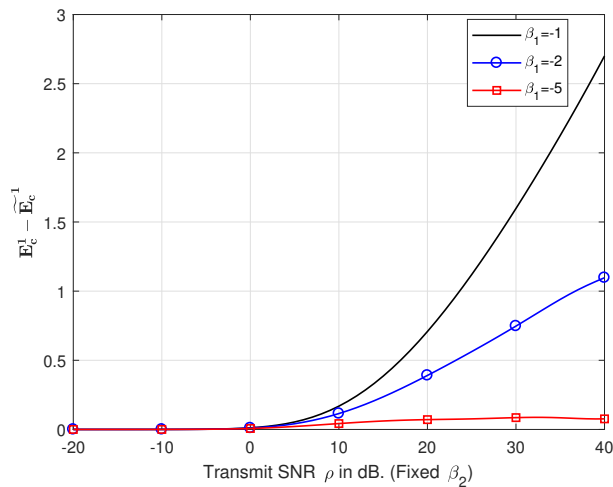


Fig. 7. $E_c^1 - \widetilde{E}_c^1$ versus ρ , for several values of the normalized delay exponent.

in the high SNR regime ($\rho = 30$ dB) as functions of the (negative) normalized delay exponent, for NOMA and OMA. We noticed that the EC curves are identical. On the other hand, in Fig.6, where E_c^1 and E_c^2 are depicted across different SNR values, $\rho \in \{1, 10, 30, 40, 50\}$ dB, as functions of the (negative) normalized delay exponent, the EC of both users increase with the transmit SNR ρ increasing.

Fig. 7 shows $E_c^1 - \widetilde{E}_c^1$ versus the transmit SNR. This curve initially starts at zero, increases at the high transmit SNRs. Also, we can note that this gap decreases with delay constraints becoming more stringent (β decreasing). This confirms **Lemma 2**.

Fig. 8 shows $E_c^2 - \widetilde{E}_c^2$ versus the transmit SNR. This curve initially starts at zero, increases to a certain maximum and starts decreasing without bound at high values of the transmit SNR. This confirms **Lemma 3**. We note that the maximum of these curves decreases when the delay becomes more stringent.

Furthermore, as the negative delay exponent decreases, the zero crossing point moves to higher SNRs; this implies that as the delay QoS constraints become more stringent, the region of SNRs over which NOMA outperforms OMA increases.

To investigate the impact of ρ on the performance of the total EC for the two-user system, in Fig.9, the plots for V_N in NOMA and V_O in OMA, versus the transmit SNR are depicted for various delay exponents. The curves demonstrate that for both NOMA and OMA, the total EC for the two users starts at the initial value of 0 and then increases with the transmit SNR, as outlined in **Lemma 4**. When ρ is very small, the total EC for the two users in NOMA, V_N , increases faster than V_O in OMA. On the contrary, with the increase of the transmit SNR, V_O becomes gradually higher than V_N . At very high values of the transmit SNR, the gap between V_N and V_O increases further. Finally, when the delay becomes more stringent, both V_N and V_O decrease.

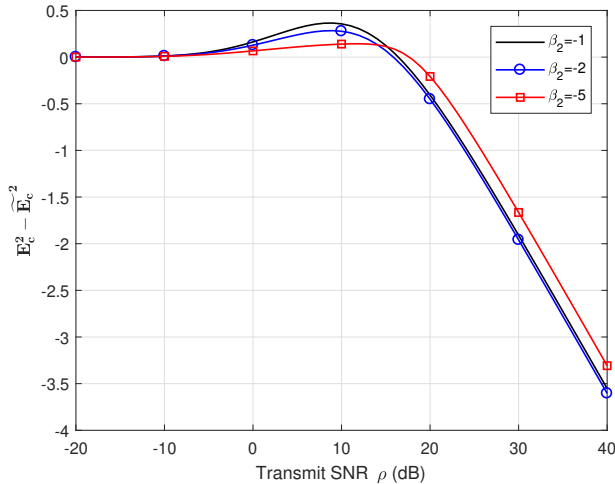


Fig. 8. $E_c^2 - \widetilde{E}_c^2$ versus ρ , for various values of normalized delay exponent.

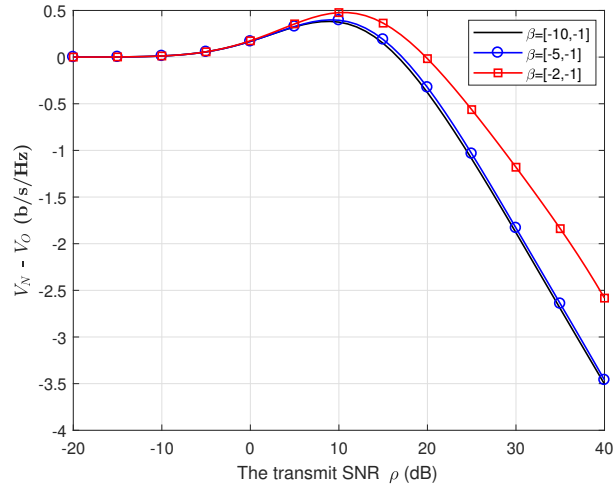


Fig. 10. $V_N - V_O$ versus ρ for various values of normalized delay exponent.

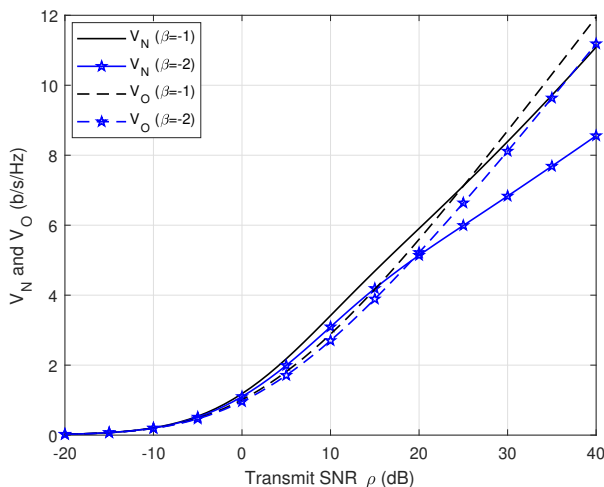


Fig. 9. V_N and V_O versus ρ , for various values of normalized delay exponent.

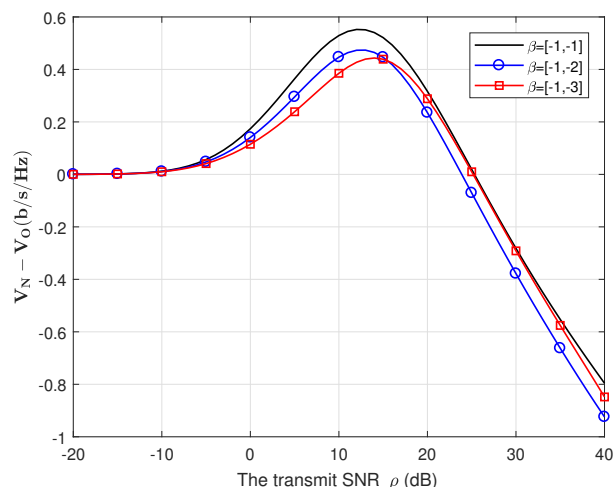


Fig. 11. $V_N - V_O$ versus ρ for various values of normalized delay exponent.

Fig.10 and Fig.11 depict $V_N - V_O$ versus ρ , for several values of the (negative) normalized delay exponent. In Fig.10, the delay of U_2 is fixed, while the delay exponent of U_1 varies. It is shown that in that case, the smallest delay QoS (i.e., the highest negative normalized delay exponent) of U_1 corresponds to the highest gap in $V_N - V_O$. With more stringent delay constraints for U_1 , NOMA outperforms OMA in an increasing region of SNRs. On the other hand, when the delay of U_1 is fixed, Fig.11 shows that the smallest delay QoS (i.e., the highest negative normalized delay exponent) for U_2 corresponds to the largest gap in $V_N - V_O$. The curve of $V_N - V_O$, initially starts at zero, increases to a maximum, and returns to negative values. In the regions in which it is positive, NOMA outperforms OMA in terms of the total EC; the opposite is true in the regions in which it is negative.

Next, we focus on the comparison of multiple NOMA pairs and OMA, i.e., E_c^{tot} and \widetilde{E}_c^{tot} . Fig. 12-(a) depicts the curves of \widetilde{E}_c^{tot} and E_c^{tot} , versus the transmit SNR. NOMA with

multiple pairs outperforms OMA. The performance gain of NOMA with multiple pairs over OMA starts at zero, increases at small values of SNR, and stabilizes at high transmit SNRs.

Fig. 12-(b) shows the curves of $E_c^{tot} - \widetilde{E}_c^{tot}$ versus the transmit SNR, for various settings of user-pairing. Initially these start at zero at low transmit SNRs, increasing to a maximum at high values of ρ . This confirms **Lemma 6**. Specifically, we set the total number of users $M = 4$; the normalized delay of all users are assumed to be equal $\beta_{1,i} = \beta_{2,i} = -1$, ($i = 1, \dots, \frac{M}{2}$). The best pairing policy in the case of $M = 4$ is (1,4)-(2,3). We noticed that even the worst pairing strategy outperforms OMA in terms of the total EC.

Fig. 13 depicts the result of the exhaustive search, done in order to find the pairing strategy which gives the highest total EC in the case of $M = 6$. The curves are normalized to the worst pairing. It appears that when these six users are divided in three groups of two users, the pairing strategy: (1,6)-(2,5)-

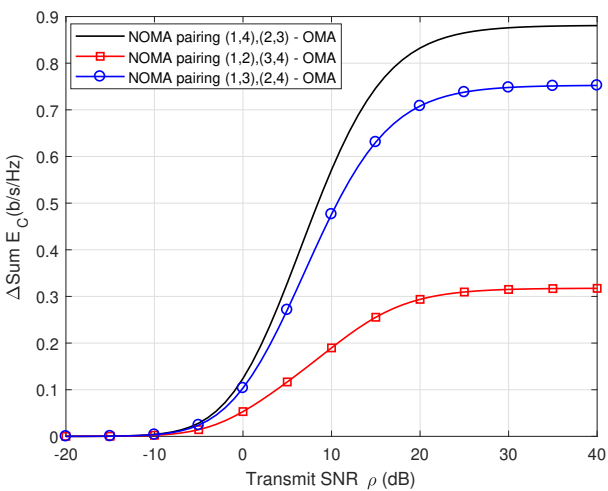
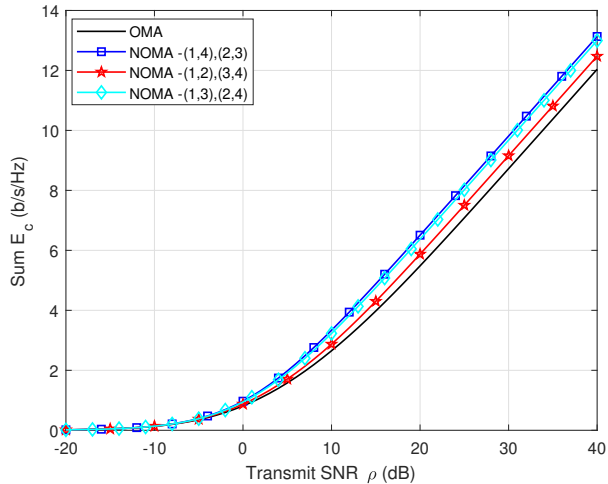


Fig. 12. (a): E_c^{tot} and \widetilde{E}_c^{tot} ; (b): $E_c^{tot} - \widetilde{E}_c^{tot}$ versus ρ for various pairing settings. $M = 4$.

(3,4) gives the highest total sum EC. We believe that this is due to the fact that coupling the strongest user and the weakest user produces the lowest interference at decoding.

Fig. 14, on the other hand, depicts the result of the exhaustive search, of valid pairs, when all six users are divided in two groups of three users. It appears that the best pairing policy in terms of total sum EC is : (1,2,6)-(3,4,5). The results for the best pairing are aligned with the literature on NOMA user pairing without delay constraints.

Fig. 15 depicts a comparison between full NOMA, i.e., when all users transmit in the same resource block, NOMA user-pairing, NOMA user-grouping (groups of 3 users) and OMA, for $M = 6$ users. Considering the best power allocation policies in the case of user-pairing and user-grouping, it appears that full NOMA outperforms all of them in terms of the total EC, followed by NOMA with user-grouping, assuming absence of error propagation due to decoding errors.

In the simulation results given above, the user pairing is presented for a specific values of the system parameters and can be further improved by the power allocation optimization, which in the present was ignored to simplify the analysis. We

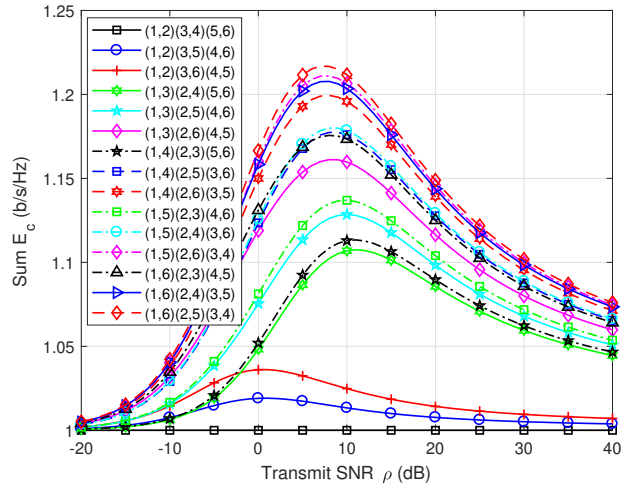


Fig. 13. E_c^{tot} versus ρ for various pairing settings, normalized to the worst pairing which is (1,2)(3,4)(5,6). $M = 6$.

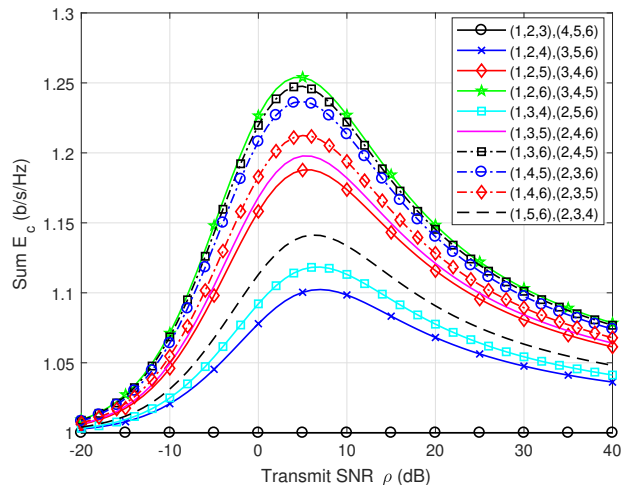


Fig. 14. Sum EC versus ρ for various grouping settings, normalized to the worst grouping which is (1,2,3)(4,5,6). $M = 6$.

note in passing that when the number of users M is not a multiple of two or three, a hybrid pairing can be used, i.e., using both clusters of two and three users.

VI. CONCLUSIONS AND FUTURE WORK

The concept of EC enabled us to study the performance gain of NOMA over OMA in systems with statistical delay QoS constraints. First, we investigated the EC of the uplink of a two-user NOMA network, assuming a Rayleigh block fading channel. We derived novel closed-form expressions for the ECs of the two users and provided a comparison between NOMA and OMA. The results show that, the EC of U_1 can surpass the EC of U_2 , as the latter is limited due to interference. Furthermore, we showed that the ECs of both users decrease as the delay constraints become more stringent. For both users, when the delay QoS of one of them is fixed, the smallest

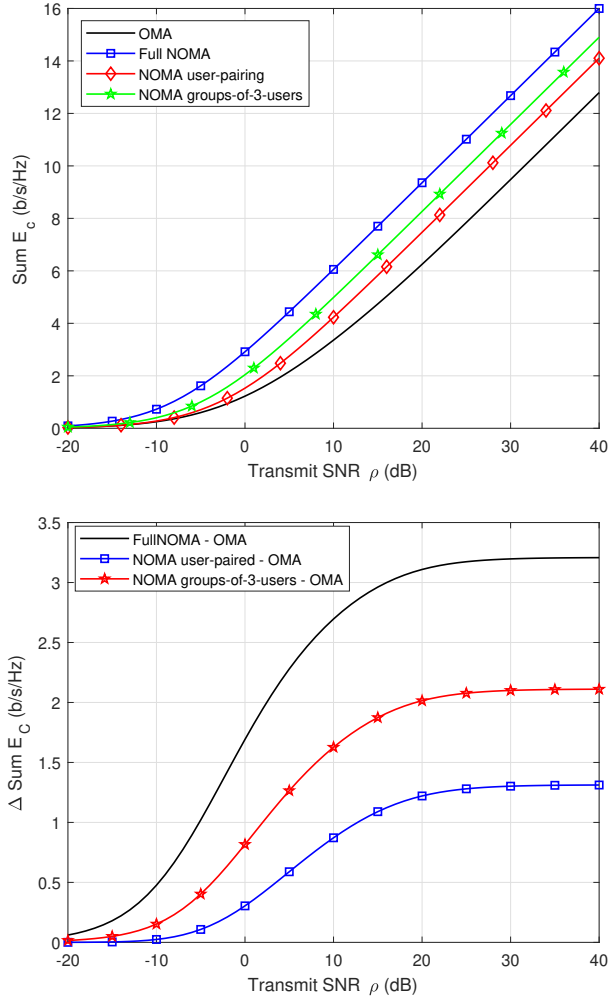


Fig. 15. Sum EC and Δ Sum EC for various setting versus ρ . $M = 6$.

values of the other's delay QoS give the highest performance gap between NOMA and OMA in terms of total EC. On the other hand, we investigated NOMA with user pairing and found the optimal pairing strategy that gave the highest EC, for $M = 4$ and $M = 6$. It turns out that NOMA grouping and NOMA pairing does not do better than full NOMA, but one can get close to it when users transmit with optimal power. NOMA with user pairing is interesting as it can be an alternative to mitigate interference on stronger users and reduce the impact of error propagation. These results raise questions on the possibility of switching between NOMA and OMA according to the individual users' delay constraints and transmit power.

APPENDIX I

$$E_c^1 = \frac{1}{\beta_1} \log_2 \left(2 \int_0^\infty (1 + \rho P_1 x_1)^{\beta_1} e^{-2x_1} dx_1 \right). \quad (29)$$

Set $t = \rho P_1 x_1$ i.e., $x_1 = \frac{t}{\rho P_1}$ and since $x_1 : 0 \rightarrow \infty \implies t : 0 \rightarrow \infty$, $dx_1 = \frac{1}{\rho P_1} dt$, we can get that:

$$E_c^1 = \frac{1}{\beta_1} \log_2 \left(\frac{2}{P_1 \rho} \int_0^\infty (1+t)^{\beta_1} e^{-\frac{2t}{P_1 \rho}} dt \right). \quad (30)$$

Also, by setting $a = 1$, $(b-a-1) = \beta_1$, $\implies b = \beta_2 + 2$, $z = \frac{2}{P_1 \rho}$ and denoting by $U(\cdot, \cdot, \cdot)$ the confluent hypergeometric function: $U(a, b, z) = \frac{1}{\Gamma(a)} \int_0^\infty e^{-zt} t^{a-1} (1+t)^{b-a-1} dt$, we have that: $\int_0^\infty (1+t)^{\beta_1} e^{-\frac{2t}{P_1 \rho}} dt = U\left(1, 2 + \beta_1, \frac{2}{\rho P_1}\right)$, which means that:

$$E_c^1 = \frac{1}{\beta_1} \log_2 \left(\frac{2}{P_1 \rho} \times U\left(1, 2 + \beta_1, \frac{2}{\rho P_1}\right) \right). \quad (31)$$

For the U_2 , we have that:

$$\begin{aligned} E_c^2 &= \frac{1}{\beta_2} \log_2 \left(\mathbb{E} \left[\left(1 + \frac{\rho P_2 x_2}{1 + \rho P_1 x_1} \right)^{\beta_2} \right] \right) \\ &= \frac{1}{\beta_2} \log_2 \left(2 \int_0^\infty \left(\frac{\rho P_2}{1 + \rho P_1 x_1} \right)^{\beta_2} e^{-x_1} \int_{x_1}^\infty \left(\frac{1 + \rho P_1 x_1}{\rho P_2} + x_2 \right)^{\beta_2} e^{-x_2} dx_2 dx_1 \right). \end{aligned} \quad (32)$$

We set $z = \frac{1 + \rho P_1 x_1}{\rho P_2} + x_2$, i.e., we have that: $x_2 = z - \frac{1 + \rho P_1 x_1}{\rho P_2}$ and $dx_2 = dz$, so that $x_2 \rightarrow x_1$, $\implies z \rightarrow \frac{1 + \rho P_1 x_1}{\rho P_2} + x_1 = \frac{1 + \rho x_1}{\rho P_2}$ and $x_2 \rightarrow \infty \implies z \rightarrow \infty$.

$$\begin{aligned} E_c^2 &= \frac{1}{\beta_2} \log_2 \left(2 \int_0^\infty \left(\frac{\rho P_2}{1 + \rho P_1 x_1} \right)^{\beta_2} e^{-x_1} \int_{\frac{1 + \rho x_1}{\rho P_2}}^\infty z^{\beta_2} e^{-\left(z - \frac{1 + \rho P_1 x_1}{\rho P_2}\right)} dz dx_1 \right) \\ &= \frac{1}{\beta_2} \log_2 \left(2 e^{\frac{x_1}{\rho P_2}} \int_0^\infty \left(\frac{\rho P_2}{1 + \rho P_1 x_1} \right)^{\beta_2} e^{-x_1} e^{\frac{P_1 x_1}{P_2}} \int_{\frac{1 + \rho x_1}{\rho P_2}}^\infty z^{\beta_2} e^{-z} dz dx_1 \right). \end{aligned} \quad (33)$$

We note that: $\int_a^\infty \frac{e^{-x}}{x^b} dx = a^{-\frac{b}{2}} e^{-\frac{a}{2}} \mathbb{W}_{-\frac{b}{2}, \frac{1-b}{2}}(a)$ where \mathbb{W} is the Whittaker \mathbb{W} function. Hence, we get that:

$$\begin{aligned} E_c^2 &= \frac{1}{\beta_2} \log_2 \left(2 e^{\frac{x_1}{\rho P_2}} \int_0^\infty \left(\frac{\rho P_2}{1 + \rho P_1 x_1} \right)^{\beta_2} e^{-x_1} e^{\frac{P_1 x_1}{P_2}} \left[\left(\frac{1 + \rho x_1}{\rho P_2} \right)^{\frac{\beta_2}{2}} e^{-\frac{1 + \rho x_1}{2\rho P_2}} \mathbb{W}_{\frac{\beta_2}{2}, \frac{1 + \beta_2}{2}} \left(\frac{1 + \rho x_1}{\rho P_2} \right) \right] dx_1 \right) \\ &= \frac{1}{\beta_2} \log_2 \left(2 (\rho P_2)^{\frac{\beta_2}{2}} e^{\frac{x_1}{2\rho P_2}} \int_0^\infty (1 + \rho P_1 x_1)^{-\beta_2} (1 + \rho x_1)^{\frac{\beta_2}{2}} e^{\frac{(2P_1 - 2P_2 - 1)x_1}{2P_2}} \left[\mathbb{W}_{\frac{\beta_2}{2}, \frac{1 + \beta_2}{2}} \left(\frac{1 + \rho x_1}{\rho P_2} \right) \right] dx_1 \right). \end{aligned} \quad (34)$$

Note that $\mathbb{W}_{u-\frac{1}{2}, u}(z) = e^{\frac{1}{2}z} z^{\frac{1}{2}-u} \Gamma(2u, z)$, so that we have $\mathbb{W}_{\frac{\beta_2}{2}, \frac{1 + \beta_2}{2}} \left(\frac{1 + \rho x_1}{\rho P_2} \right) = e^{\frac{1 + \rho x_1}{2\rho P_2}} \left(\frac{1 + \rho x_1}{\rho P_2} \right)^{-\frac{\beta_2}{2}} \Gamma\left(1 + \beta_2, \frac{1 + \rho x_1}{\rho P_2}\right)$.

By substituting it in E_c^2 , we have that:

$$E_c^2 = \frac{1}{\beta_2} \log_2 \left(2(\rho P_2)^{\beta_2} e^{\frac{1}{\rho P_2}} \int_0^\infty (1 + \rho P_1 x_1)^{-\beta_2} e^{\frac{(P_1 - P_2)x_1}{P_2}} \times \Gamma \left(1 + \beta_2, \frac{1 + \rho x_1}{\rho P_2} \right) dx_1 \right). \quad (35)$$

To continue we set $\frac{1 + \rho x_1}{\rho P_2} = y$, i.e., $x_1 = P_2 y - \frac{1}{\rho}$, and $dx_1 = P_2 dy$. $x_1 \rightarrow 0 \implies y \rightarrow \frac{1}{\rho P_2}$ and $x_1 \rightarrow \infty \implies y \rightarrow \infty$. Recall that without loss of generality we have set $P_1 + P_2 = 1$. Then we get that

$$\begin{aligned} E_c^2 &= \frac{1}{\beta_2} \log_2 \left(2(\rho P_2)^{\beta_2} e^{\frac{1}{\rho P_2}} \int_0^\infty (1 + \rho P_1 x_1)^{-\beta_2} \right. \\ &\quad \times e^{\frac{(P_1 - P_2)x_1}{P_2}} \left[\Gamma \left(1 + \beta_2, \frac{1 + \rho x_1}{\rho P_2} \right) \right] dx_1 \Big) \\ &= \frac{1}{\beta_2} \log_2 \left(2P_2 (\rho P_2)^{\beta_2} e^{\frac{1}{\rho P_2}} e^{-\frac{(P_1 - P_2)}{\rho P_2}} \right. \\ &\quad \times \int_{\frac{1}{\rho P_2}}^\infty P_2^{-\beta_2} (1 + \rho P_1 y)^{-\beta_2} e^{(P_1 - P_2)y} \Gamma(1 + \beta_2, y) dy \Big). \end{aligned} \quad (36)$$

Using binomial expansion we have $(1 + \rho P_1 y)^{-\beta_2} = \sum_{j=0}^{-\beta_2} \binom{-\beta_2}{j} (\rho P_1 y)^j$ when β_2 is integer, otherwise we use $[\beta_2]$. And, using Taylor series expansion we have that $e^{(P_1 - P_2)y} = e^{-(P_2 - P_1)y} = \sum_{k=0}^\infty \frac{(-1)^k (P_2 - P_1)^k}{k!} y^k$, which converges.

$$\begin{aligned} E_c^2 &= \frac{1}{\beta_2} \log_2 \left(2P_2^{1-\beta_2} (\rho P_2)^{\beta_2} e^{\frac{1}{\rho P_2}} e^{-\frac{(P_1 - P_2)}{\rho P_2}} \right. \\ &\quad \times \int_{\frac{1}{\rho P_2}}^\infty (1 + \rho P_1 y)^{-\beta_2} e^{(P_1 - P_2)y} \Gamma(1 + \beta_2, y) dy \Big) \\ &= \frac{1}{\beta_2} \log_2 \left(2P_2^{1-\beta_2} (\rho P_2)^{\beta_2} e^{\frac{1}{\rho P_2}} e^{-\frac{(P_1 - P_2)}{\rho P_2}} \right. \\ &\quad \times \sum_{j=0}^{-\beta_2} \binom{-\beta_2}{j} (\rho P_1)^j \times \sum_{k=0}^\infty \frac{(-1)^k (P_2 - P_1)^k}{k!} \\ &\quad \times \int_{\frac{1}{\rho P_2}}^\infty y^{j+k} \Gamma(1 + \beta_2, y) dy \Big). \end{aligned} \quad (37)$$

Note that

$$\int_c^\infty z^b \Gamma(A, z) dz = \frac{1}{1+b} \left(-c^{1+b} \Gamma(A, c) + \Gamma(1 + A + b, c) \right)$$

i.e.,

$$\begin{aligned} \int_{\frac{1}{\rho P_2}}^\infty y^{j+k} \Gamma(1 + \beta_2, y) dy &= \frac{1}{1 + j + k} \\ &\times \left(-(\rho P_2)^{-1-j-k} \Gamma(1 + \beta_2, \frac{1}{\rho P_2}) + \Gamma(2 + \beta_2 + j + k, \frac{1}{\rho P_2}) \right). \end{aligned} \quad (38)$$

Finally, by inserting (38) in (37) we obtain (12).

APPENDIX II

By inserting $\rho \rightarrow 0$ into (11) and (12), we get 1) of **Lemma I**, i.e.,

$$\lim_{\rho \rightarrow 0} (E_c^1 - \tilde{E}_c^1) = \frac{1}{\beta_1} \log_2 \left(\frac{\mathbb{E} \left[(1 + \rho P_1 |h_1|^2)^{\beta_2} \right]}{\mathbb{E} \left[(1 + 2\rho P_1 |h_1|^2)^{\frac{\beta_2}{2}} \right]} \right) = 0,$$

$$\lim_{\rho \rightarrow 0} (E_c^2 - \tilde{E}_c^2) = \frac{1}{\beta_2} \log_2 \left(\frac{\mathbb{E} \left[\left(1 + \frac{\rho P_2 |h_2|^2}{1 + \rho P_1 |h_1|^2} \right)^{\beta_2} \right]}{\mathbb{E} \left[(1 + 2\rho P_2 |h_1|^2)^{\frac{\beta_2}{2}} \right]} \right) = 0.$$

In the same way, by inserting $\rho \rightarrow \infty$ into (11) and (12), we get 2) in **Lemma I**, given below.

$$\begin{aligned} \lim_{\rho \rightarrow \infty} E_c^2 &= \frac{1}{\beta_2} \log_2 \left(\mathbb{E} \left[\left(1 + \frac{P_2 |h_2|^2}{P_1 |h_1|^2} \right)^{\beta_2} \right] \right), \\ \lim_{\rho \rightarrow \infty} (E_c^1 - \tilde{E}_c^1) &= \frac{1}{\beta_1} \log_2 \left((\rho P_1)^{\frac{\beta_1}{2}} \frac{\mathbb{E} \left[\left(\frac{1}{\rho P_1} + |h_1|^2 \right)^{\beta_2} \right]}{\mathbb{E} \left[\left(\frac{1}{\rho P_1} + 2|h_1|^2 \right)^{\frac{\beta_2}{2}} \right]} \right) \\ &= \infty, \\ \lim_{\rho \rightarrow \infty} (E_c^2 - \tilde{E}_c^2) &= \frac{1}{\beta_2} \log_2 \left(\frac{\mathbb{E} \left[\left(\frac{\frac{1}{\rho} + P_1 |h_1|^2 + P_2 |h_2|^2}{\frac{1}{\rho} + P_1 |h_1|^2} \right)^{\beta_2} \right]}{\rho^{\frac{\beta_2}{2}} \mathbb{E} \left[\left(\frac{1}{\rho} + 2P_2 |h_2|^2 \right)^{\frac{\beta_2}{2}} \right]} \right) \\ &= -\infty. \end{aligned}$$

APPENDIX III

To analyze the trends of E_c^1 and \tilde{E}_c^1 with respect to ρ , we start with

$$\begin{aligned} \frac{\partial E_c^1}{\partial \rho} &= \frac{1}{\beta_1 \ln 2} \frac{\left(\mathbb{E}[(1 + \rho P_1 |h_1|^2)^{\beta_1}] \right)'}{\mathbb{E}[(1 + \rho P_1 |h_1|^2)^{\beta_1}]} \\ &= \frac{P_1 \mathbb{E}[|h_1|^2 (1 + \rho P_1 |h_1|^2)^{\beta_1 - 1}]}{\ln 2 \mathbb{E}[(1 + \rho P_1 |h_1|^2)^{\beta_1}]} \geq 0. \end{aligned} \quad (39)$$

Similarly, for U_1 in OMA we have that

$$\begin{aligned} \frac{\partial \tilde{E}_c^1}{\partial \rho} &= \frac{1}{\beta_1 \ln 2} \frac{\left(\mathbb{E}[(1 + 2\rho P_1 |h_1|^2)^{\frac{\beta_1}{2}}] \right)'}{\mathbb{E}[(1 + 2\rho P_1 |h_1|^2)^{\frac{\beta_1}{2}}]} \\ &= \frac{P_1 \mathbb{E}[|h_1|^2 (1 + 2\rho P_1 |h_1|^2)^{\frac{\beta_1}{2} - 1}]}{\ln 2 \mathbb{E}[(1 + 2\rho P_1 |h_1|^2)^{\frac{\beta_1}{2}}]} \geq 0. \end{aligned} \quad (40)$$

Then, we get that

$$\begin{aligned} \frac{\partial (E_c^1 - \tilde{E}_c^1)}{\partial \rho} &= \frac{P_1 \mathbb{E}[|h_1|^2 (1 + \rho P_1 |h_1|^2)^{\beta_1 - 1}]}{\ln 2 \mathbb{E}[(1 + \rho P_1 |h_1|^2)^{\beta_1}]} \\ &\quad - \frac{P_1 \mathbb{E}[|h_1|^2 (1 + 2\rho P_1 |h_1|^2)^{\frac{\beta_1}{2} - 1}]}{\ln 2 \mathbb{E}[(1 + 2\rho P_1 |h_1|^2)^{\frac{\beta_1}{2}}]}. \end{aligned} \quad (41)$$

and $\lim_{\rho \rightarrow 0} \left(\frac{\partial(E_c^1 - \tilde{E}_c^1)}{\partial \rho} \right) = \frac{(P_1 - P_1)}{\ln 2} \mathbb{E}[|h_1|^2] = 0$. When $\rho \gg 1$, we have that

$$\begin{aligned} \frac{\partial(E_c^1 - \tilde{E}_c^1)}{\partial \rho} &= \frac{P_1}{\rho \ln 2} \frac{\mathbb{E}[|h_1|^2 (P_1 |h_1|^2)^{\beta_1 - 1}]}{\mathbb{E}[(P_1 |h_1|^2)^{\beta_1}]} \\ &\quad - \frac{P_1}{\rho \ln 2} \frac{\mathbb{E}[|h_1|^2 (2P_1 |h_1|^2)^{\frac{\beta_1}{2} - 1}]}{\mathbb{E}[(2P_1 |h_1|^2)^{\frac{\beta_1}{2}}]} \\ &= \frac{1}{2\rho \ln 2} \geq 0. \end{aligned} \quad (42)$$

When $\rho \rightarrow \infty$, this term approaches 0.

APPENDIX IV

$$E_c^2 = \frac{1}{\beta_2} \log_2 \left(\mathbb{E} \left[\left(1 + \frac{\rho P_2 |h_2|^2}{1 + \rho P_1 |h_1|^2} \right)^{\beta_2} \right] \right). \quad (43)$$

And

$$\begin{aligned} \frac{\partial E_c^2}{\partial \rho} &= \frac{1}{\beta_2 \ln 2} \frac{\left(\mathbb{E} \left[\left(1 + \frac{\rho P_2 |h_2|^2}{1 + \rho P_1 |h_1|^2} \right)^{\beta_2} \right] \right)'}{\mathbb{E} \left[\left(1 + \frac{\rho P_2 |h_2|^2}{1 + \rho P_1 |h_1|^2} \right)^{\beta_2} \right]} \\ &= \frac{1}{\ln 2} \frac{\mathbb{E} \left[\frac{P_2 |h_2|^2}{(1 + \rho P_1 |h_1|^2)^2} \left(1 + \frac{\rho P_2 |h_2|^2}{1 + \rho P_1 |h_1|^2} \right)^{\beta_2 - 1} \right]}{\mathbb{E} \left[\left(1 + \frac{\rho P_2 |h_2|^2}{1 + \rho P_1 |h_1|^2} \right)^{\beta_2} \right]} \geq 0. \end{aligned} \quad (44)$$

In the same way, for the U_2 in OMA, we have that:

$$\begin{aligned} \frac{\partial \tilde{E}_c^2}{\partial \rho} &= \frac{1}{\beta_2 \ln 2} \frac{\left(\mathbb{E}[(1 + 2\rho P_2 |h_2|^2)^{\frac{\beta_2}{2}}] \right)'}{\mathbb{E}[(1 + 2\rho P_2 |h_2|^2)^{\frac{\beta_2}{2}}]} \\ &= \frac{P_2}{\ln 2} \frac{\mathbb{E}[|h_2|^2 (1 + 2\rho P_2 |h_2|^2)^{\frac{\beta_2}{2} - 1}]}{\mathbb{E}[(1 + 2\rho P_2 |h_2|^2)^{\frac{\beta_2}{2}}]} \geq 0, \end{aligned} \quad (45)$$

and

$$\begin{aligned} \frac{\partial(E_c^2 - \tilde{E}_c^2)}{\partial \rho} &= \frac{1}{\ln 2} \frac{\mathbb{E} \left[\frac{P_2 |h_2|^2}{(1 + \rho P_1 |h_1|^2)^2} \left(1 + \frac{\rho P_2 |h_2|^2}{1 + \rho P_1 |h_1|^2} \right)^{\beta_2 - 1} \right]}{\mathbb{E} \left[\left(1 + \frac{\rho P_2 |h_2|^2}{1 + \rho P_1 |h_1|^2} \right)^{\beta_2} \right]} \\ &\quad - \frac{P_2}{\ln 2} \frac{\mathbb{E}[|h_2|^2 (1 + 2\rho P_2 |h_2|^2)^{\frac{\beta_2}{2} - 1}]}{\mathbb{E}[(1 + 2\rho P_2 |h_2|^2)^{\frac{\beta_2}{2}}]}. \end{aligned} \quad (46)$$

When $\rho \rightarrow 0$, we have that $\lim_{\rho \rightarrow 0} \left(\frac{\partial(E_c^2 - \tilde{E}_c^2)}{\partial \rho} \right) = 0$. When ρ is very large,

$$\begin{aligned} \frac{\partial(E_c^2 - \tilde{E}_c^2)}{\partial \rho} &= \frac{\mathbb{E} \left[\frac{P_2 |h_2|^2}{\rho^2 \left(\frac{1}{\rho} + P_1 |h_1|^2 \right)^2} \left(1 + \frac{\rho P_2 |h_2|^2}{\rho \left(\frac{1}{\rho} + P_1 |h_1|^2 \right)} \right)^{\beta_2 - 1} \right]}{\ln 2 \mathbb{E} \left[\left(1 + \frac{\rho P_2 |h_2|^2}{\rho \left(\frac{1}{\rho} + P_1 |h_1|^2 \right)} \right)^{\beta_2} \right]} \\ &\quad - \frac{P_2}{\ln 2} \frac{1}{\rho} \frac{\mathbb{E}[|h_2|^2 \left(\frac{1}{\rho} + 2P_2 |h_2|^2 \right)^{\frac{\beta_2}{2} - 1}]}{\mathbb{E}[\left(\frac{1}{\rho} + 2P_2 |h_2|^2 \right)^{\frac{\beta_2}{2}}]} \\ &= \frac{P_2}{\rho^2 P_1^2 \ln 2} \frac{\mathbb{E} \left[\frac{|h_2|^2}{(|h_1|^2)^2} \left(1 + \frac{P_2 |h_2|^2}{P_1 |h_1|^2} \right)^{\beta_2 - 1} \right]}{\mathbb{E} \left[\left(1 + \frac{P_2 |h_2|^2}{P_1 |h_1|^2} \right)^{\beta_2} \right]} - \frac{1}{2 \ln 2} \frac{1}{\rho} \\ &= \frac{P_2}{P_1^2 \ln 2} A - \frac{1}{2 \ln 2} \frac{1}{\rho}, \end{aligned} \quad (47)$$

where $A = \frac{\mathbb{E} \left[\frac{|h_2|^2}{(|h_1|^2)^2} \left(1 + \frac{P_2 |h_2|^2}{P_1 |h_1|^2} \right)^{\beta_2 - 1} \right]}{\mathbb{E} \left[\left(1 + \frac{P_2 |h_2|^2}{P_1 |h_1|^2} \right)^{\beta_2} \right]}$, unrelated to ρ . And it gradually approaches 0 when $\rho \rightarrow \infty$.

APPENDIX V

Note that $V_N = E_c^1 + E_c^2$. By using **Lemma 1**, we have that $\lim_{\rho \rightarrow 0} (V_N) = 0$ and $\lim_{\rho \rightarrow \infty} (V_N) = \infty$. Then, we get that,

$$\begin{aligned} \frac{\partial V_N}{\partial \rho} &= \frac{\partial(E_c^1 + E_c^2)}{\partial \rho} = \frac{P_1}{\ln 2} \frac{\mathbb{E}[|h_1|^2 (1 + \rho P_1 |h_1|^2)^{\beta_1 - 1}]}{\mathbb{E}[(1 + \rho P_1 |h_1|^2)^{\beta_1}]} \\ &\quad + \frac{1}{\ln 2} \frac{\mathbb{E} \left[\frac{P_2 |h_2|^2}{(1 + \rho P_1 |h_1|^2)^2} \left(1 + \frac{\rho P_2 |h_2|^2}{1 + \rho P_1 |h_1|^2} \right)^{\beta_2 - 1} \right]}{\mathbb{E} \left[\left(1 + \frac{\rho P_2 |h_2|^2}{1 + \rho P_1 |h_1|^2} \right)^{\beta_2} \right]} \geq 0. \end{aligned} \quad (48)$$

When $\rho \rightarrow 0$, we have that $\lim_{\rho \rightarrow 0} \left(\frac{\partial V_N}{\partial \rho} \right) = \frac{P_1}{\ln 2} \mathbb{E}[|h_1|^2] + \frac{P_2}{\ln 2} \mathbb{E}[|h_2|^2]$.

When $\rho \rightarrow \infty$, we get that

$$\lim_{\rho \rightarrow \infty} \frac{\partial V_N}{\partial \rho} = \frac{1}{\rho \ln 2} + \frac{\mathbb{E} \left[\frac{P_2 |h_2|^2}{(P_1 |h_1|^2)^2} \left(1 + \frac{P_2 |h_2|^2}{P_1 |h_1|^2} \right)^{\beta_2 - 1} \right]}{\rho^2 \ln 2 \mathbb{E} \left[\left(1 + \frac{P_2 |h_2|^2}{P_1 |h_1|^2} \right)^{\beta_2} \right]} = 0.$$

For V_O in the case of OMA, we note that $V_O = \tilde{E}_c^1 + \tilde{E}_c^2$. By using **Lemma 1**, we have $\lim_{\rho \rightarrow 0} (V_O) = 0$ and $\lim_{\rho \rightarrow \infty} (V_O) = \infty$. Then,

$$\begin{aligned} \frac{\partial V_O}{\partial \rho} &= \frac{\partial(\tilde{E}_c^1 + \tilde{E}_c^2)}{\partial \rho} = \frac{P_1}{\ln 2} \frac{\mathbb{E}[|h_1|^2 (1 + 2\rho P_1 |h_1|^2)^{\frac{\beta_1}{2} - 1}]}{\mathbb{E}[(1 + 2\rho P_1 |h_1|^2)^{\frac{\beta_1}{2}}]} \\ &\quad + \frac{P_2}{\ln 2} \frac{\mathbb{E}[|h_2|^2 (1 + 2\rho P_2 |h_2|^2)^{\frac{\beta_2}{2} - 1}]}{\mathbb{E}[(1 + 2\rho P_2 |h_2|^2)^{\frac{\beta_2}{2}}]} \geq 0. \end{aligned} \quad (49)$$

When $\rho \rightarrow 0$, we have that $\lim_{\rho \rightarrow 0} \left(\frac{\partial V_O}{\partial \rho} \right) = \frac{P_1}{\ln 2} \mathbb{E}[|h_1|^2] + \frac{P_2}{\ln 2} \mathbb{E}[|h_2|^2]$. When $\rho \rightarrow \infty$, we have that $\lim_{\rho \rightarrow \infty} \left(\frac{\partial V_O}{\partial \rho} \right) = \lim_{\rho \rightarrow \infty} \left(\frac{1}{2\rho \ln 2} + \frac{1}{2\rho \ln 2} \right) = \lim_{\rho \rightarrow \infty} \left(\frac{1}{\rho \ln 2} \right)$, which equals to 0.

APPENDIX VI

We have

$$\begin{aligned} E_c^2 &= \frac{1}{\beta_2} \log_2 \left(\mathbb{E} \left[\left(1 + \frac{\rho P_2 |h_2|^2}{1 + \rho P_1 |h_1|^2} \right)^{\beta_2} \right] \right) \\ &= -\frac{1}{\theta_2 T_f B} \left(\mathbb{E} \left[-\frac{\theta_2 T_f B}{\ln 2} \ln \left(1 + \frac{\rho P_2 |h_2|^2}{1 + \rho P_1 |h_1|^2} \right) \right] \right). \end{aligned} \quad (50)$$

When $\theta_2 \rightarrow 0$, we get an indeterminate form. By applying the L'Hopital's rule one can get

$$\begin{aligned} E_c^2 &= -\frac{1}{T_f B} \left(\mathbb{E} \left[-\frac{T_f B}{\ln 2} \ln \left(1 + \frac{\rho P_2 |h_2|^2}{1 + \rho P_1 |h_1|^2} \right) \right] \right) \\ &= \mathbb{E} \left[\log_2 \left(1 + \frac{\rho P_2 |h_2|^2}{1 + \rho P_1 |h_1|^2} \right) \right]. \end{aligned} \quad (51)$$

Hence, we get that

$$\lim_{\theta_2 \rightarrow 0} E_c^2 = \mathbb{E} \left[\log_2 \left(1 + \frac{\rho P_2 |h_2|^2}{1 + \rho P_1 |h_1|^2} \right) \right],$$

which equals to $\mathbb{E}[R_2]$, the ergodic capacity.

Proceeding in the same way, one can find

$$\begin{aligned}\lim_{\theta_1 \rightarrow 0} E_c^1 &= \mathbb{E} \left[\log_2 \left(1 + \rho P_1 |h_1|^2 \right) \right] = \mathbb{E}[R_1], \\ \lim_{\theta_1 \rightarrow 0} \tilde{E}_c^1 &= \mathbb{E} \left[\frac{1}{2} \log_2 \left(1 + 2\rho P_1 |h_1|^2 \right) \right] = \mathbb{E}[\tilde{R}_1], \\ \lim_{\theta_2 \rightarrow 0} \tilde{E}_c^2 &= \mathbb{E} \left[\frac{1}{2} \log_2 \left(1 + 2\rho P_2 |h_2|^2 \right) \right] = \mathbb{E}[\tilde{R}_2], \\ \lim_{\theta_1 \rightarrow 0} (E_c^1 - \tilde{E}_c^1) &= \mathbb{E}[R_1] - \mathbb{E}[\tilde{R}_1], \\ \lim_{\theta_2 \rightarrow 0} (E_c^2 - \tilde{E}_c^2) &= \mathbb{E}[R_2] - \mathbb{E}[\tilde{R}_2].\end{aligned}$$

To look further the impact of the transmit SNR ρ on the EC considering delay-unconstrained user:

$$\lim_{\substack{\theta_1 \rightarrow 0 \\ \rho \rightarrow \infty}} E_c^1 = \lim_{\rho \rightarrow \infty} \mathbb{E} \left[\log_2 \left(1 + \rho P_1 |h_1|^2 \right) \right] = \infty,$$

We also have that

$$\begin{aligned}\lim_{\substack{\theta_2 \rightarrow 0 \\ \rho \rightarrow \infty}} E_c^2 &= \lim_{\rho \rightarrow \infty} \mathbb{E} \left[\log_2 \left(1 + \frac{\rho P_2 |h_2|^2}{1 + \rho P_1 |h_1|^2} \right) \right] \\ &= \mathbb{E} \left[\log_2 \left(1 + \frac{P_2 |h_2|^2}{P_1 |h_1|^2} \right) \right].\end{aligned}$$

Similarly, we have for OMA

$$\begin{aligned}\lim_{\substack{\theta_1 \rightarrow 0 \\ \rho \rightarrow \infty}} \tilde{E}_c^1 &= \lim_{\rho \rightarrow \infty} \mathbb{E} \left[\frac{1}{2} \log_2 \left(1 + 2\rho P_1 |h_1|^2 \right) \right] = \infty, \\ \lim_{\substack{\theta_2 \rightarrow 0 \\ \rho \rightarrow \infty}} \tilde{E}_c^2 &= \lim_{\rho \rightarrow \infty} \mathbb{E} \left[\frac{1}{2} \log_2 \left(1 + 2\rho P_2 |h_2|^2 \right) \right] = \infty.\end{aligned}$$

Therefore, we have that

$$\begin{aligned}\lim_{\substack{\theta_1 \rightarrow 0 \\ \rho \rightarrow \infty}} (E_c^1 - \tilde{E}_c^1) &= \lim_{\rho \rightarrow \infty} \left(\mathbb{E} \left[\log_2 \left(\frac{1 + \rho P_1 |h_1|^2}{(1 + 2\rho P_1 |h_1|^2)^{\frac{1}{2}}} \right) \right] \right) \\ &= \lim_{\rho \rightarrow \infty} \left(\mathbb{E} \left[\log_2 \left(\sqrt{\frac{\rho P_1 |h_1|^2}{2}} \right) \right] \right) = \infty.\end{aligned}$$

$$\lim_{\substack{\theta_2 \rightarrow 0 \\ \rho \rightarrow \infty}} (E_c^2 - \tilde{E}_c^2) = -\infty.$$

APPENDIX VII

Using the **Lemma 1**, when $\rho \rightarrow 0$, we can show that $E_c^{1,i} - \tilde{E}_c^{1,i} \rightarrow 0$ and $E_c^{2,i} - \tilde{E}_c^{2,i} \rightarrow 0$. Then $E_c^{tot} - \tilde{E}_c^{tot} \rightarrow 0$, since $E_c^{tot} - \tilde{E}_c^{tot} = \sum_{i=1}^{\frac{M}{2}} (E_c^{1,i} + E_c^{2,i} - \tilde{E}_c^{1,i} - \tilde{E}_c^{2,i})$, we get

$$\lim_{\rho \rightarrow 0} (E_c^{tot} - \tilde{E}_c^{tot}) = 0.$$

On the other side, when $\rho \rightarrow \infty$,

$$\begin{aligned}E_c^{tot} - \tilde{E}_c^{tot} &= \sum_{i=1}^{\frac{M}{2}} \left(\frac{1}{\beta_{1,i}} \log_2 \left(\frac{\mathbb{E} \left[(1 + \rho P_{1,i} |h_{1,i}|^2)^{\frac{2\beta_{1,i}}{M}} \right]}{\mathbb{E} \left[(1 + 2\rho P_{1,i} |h_{1,i}|^2)^{\frac{\beta_{1,i}}{M}} \right]} \right) \right) \\ &+ \frac{1}{\beta_{2,i}} \log_2 \left(\frac{\mathbb{E} \left[\left(1 + \frac{\rho P_{2,i} |h_{2,i}|^2}{1 + \rho P_{1,i} |h_{1,i}|^2} \right)^{\frac{2\beta_{2,i}}{M}} \right]}{\mathbb{E} \left[(1 + 2\rho P_{2,i} |h_{2,i}|^2)^{\frac{\beta_{2,i}}{M}} \right]} \right) \\ &= \sum_{i=1}^{\frac{M}{2}} \left(\frac{1}{\beta_{1,i}} \log_2 \left(\rho^{\frac{\beta_{1,i}}{M}} \frac{\mathbb{E} \left[\left(\frac{1}{\rho} + P_{1,i} |h_{1,i}|^2 \right)^{\frac{2\beta_{1,i}}{M}} \right]}{\mathbb{E} \left[\left(\frac{1}{\rho} + 2P_{1,i} |h_{1,i}|^2 \right)^{\frac{\beta_{1,i}}{M}} \right]} \right) \right) \\ &+ \frac{1}{\beta_{2,i}} \log_2 \left(\rho^{-\frac{\beta_{2,i}}{M}} \frac{\mathbb{E} \left[\left(1 + \frac{P_{2,i} |h_{2,i}|^2}{\frac{1}{\rho} + P_{1,i} |h_{1,i}|^2} \right)^{\frac{2\beta_{2,i}}{M}} \right]}{\mathbb{E} \left[\left(\frac{1}{\rho} + 2P_{2,i} |h_{2,i}|^2 \right)^{\frac{\beta_{2,i}}{M}} \right]} \right). \quad (52)\end{aligned}$$

Then,

$$\begin{aligned}E_c^{tot} - \tilde{E}_c^{tot} &= \sum_{i=1}^{\frac{M}{2}} \left(\frac{1}{\beta_{1,i}} \log_2 \left(\frac{\mathbb{E} \left[\left(\frac{1}{\rho} + P_{1,i} |h_{1,i}|^2 \right)^{\frac{2\beta_{1,i}}{M}} \right]}{\mathbb{E} \left[\left(\frac{1}{\rho} + 2P_{1,i} |h_{1,i}|^2 \right)^{\frac{\beta_{1,i}}{M}} \right]} \right) \right) \\ &+ \frac{1}{\beta_{2,i}} \log_2 \left(\frac{\mathbb{E} \left[\left(1 + \frac{P_{2,i} |h_{2,i}|^2}{\frac{1}{\rho} + P_{1,i} |h_{1,i}|^2} \right)^{\frac{2\beta_{2,i}}{M}} \right]}{\mathbb{E} \left[\left(\frac{1}{\rho} + 2P_{2,i} |h_{2,i}|^2 \right)^{\frac{\beta_{2,i}}{M}} \right]} \right). \quad (53)\end{aligned}$$

$$\begin{aligned}\lim_{\rho \rightarrow \infty} (E_c^{tot} - \tilde{E}_c^{tot}) &= \sum_{i=1}^{\frac{M}{2}} \left(\frac{1}{\beta_{1,i}} \log_2 \left(2^{-\frac{\beta_{1,i}}{M}} \mathbb{E} \left[(P_{1,i} |h_{1,i}|^2)^{\frac{\beta_{1,i}}{M}} \right] \right) \right) \\ &+ \frac{1}{\beta_{2,i}} \log_2 \left(\frac{\mathbb{E} \left[\left(1 + \frac{P_{2,i} |h_{2,i}|^2}{P_{1,i} |h_{1,i}|^2} \right)^{\frac{2\beta_{2,i}}{M}} \right]}{\mathbb{E} \left[(2P_{2,i} |h_{2,i}|^2)^{\frac{\beta_{2,i}}{M}} \right]} \right),\end{aligned}$$

which is a constant with respect to ρ .

Furthermore, to analyze $\lim_{\rho \rightarrow 0} (\frac{\partial(E_c^{tot} - \tilde{E}_c^{tot})}{\partial \rho})$ and $\lim_{\rho \rightarrow \infty} (\frac{\partial(E_c^{tot} - \tilde{E}_c^{tot})}{\partial \rho})$, we start with $\frac{\partial E_c^{tot}}{\partial \rho}$ and $\frac{\partial \tilde{E}_c^{tot}}{\partial \rho}$.

$$\begin{aligned}\frac{\partial E_c^{tot}}{\partial \rho} &= \sum_{i=1}^{\frac{M}{2}} \left(\frac{\partial E_c^{1,i}}{\partial \rho} + \frac{\partial E_c^{2,i}}{\partial \rho} \right) \\ &= \sum_{i=1}^{\frac{M}{2}} \left(\frac{2P_{1,i}}{M \ln 2} \frac{\mathbb{E} \left[|h_{1,i}|^2 (1 + \rho P_{1,i} |h_{1,i}|^2)^{\frac{2\beta_{1,i}}{M} - 1} \right]}{\mathbb{E} \left[(1 + \rho P_{1,i} |h_{1,i}|^2)^{\frac{2\beta_{1,i}}{M}} \right]} \right) \\ &+ \frac{2P_{2,i}}{M \ln 2} \frac{\mathbb{E} \left[\frac{|h_{2,i}|^2}{(1 + \rho P_{1,i} |h_{1,i}|^2)^2} \left(1 + \frac{\rho P_{2,i} |h_{2,i}|^2}{1 + \rho P_{1,i} |h_{1,i}|^2} \right)^{\frac{2\beta_{2,i}}{M} - 1} \right]}{\mathbb{E} \left[\left(1 + \frac{\rho P_{2,i} |h_{2,i}|^2}{1 + \rho P_{1,i} |h_{1,i}|^2} \right)^{\frac{2\beta_{2,i}}{M}} \right]} \right), \quad (54)\end{aligned}$$

where $(\cdot)'$ a first derivative with respect to ρ . Then, $\lim_{\rho \rightarrow 0} (\frac{\partial E_c^{tot}}{\partial \rho}) = \sum_{i=1}^{\frac{M}{2}} \left(\frac{2P_{1,i}}{M \ln 2} \mathbb{E}[|h_{1,i}|^2] + \frac{2P_{2,i}}{M \ln 2} \mathbb{E}[|h_{2,i}|^2] \right)$.

$$\lim_{\rho \rightarrow \infty} \left(\frac{\partial E_c^{tot}}{\partial \rho} \right) = \lim_{\rho \rightarrow \infty} \left(\sum_{i=1}^{\frac{M}{2}} \left(\frac{2}{M \ln 2 \rho} + \frac{2P_{2,i}}{M \ln 2 \rho^2} \frac{\mathbb{E} \left[\frac{|h_{2,i}|^2}{(P_{1,i}|h_{1,i}|^2)^2} \left(1 + \frac{P_{2,i}|h_{2,i}|^2}{P_{1,i}|h_{1,i}|^2} \right)^{\frac{2\beta_{2,i}}{M}-1} \right]}{\mathbb{E} \left[\left(1 + \frac{P_{2,i}|h_{2,i}|^2}{P_{1,i}|h_{1,i}|^2} \right)^{\frac{2\beta_{2,i}}{M}} \right]} \right) \right) = 0.$$

Similarly,

$$\begin{aligned} \frac{\partial \widetilde{E}_c^{tot}}{\partial \rho} &= \sum_{i=1}^{\frac{M}{2}} \left(\frac{\partial \widetilde{E}_c^1}{\partial \rho} + \frac{\partial \widetilde{E}_c^2}{\partial \rho} \right), \\ &= \sum_{i=1}^{\frac{M}{2}} \left(\frac{1}{M \ln 2} \frac{\mathbb{E} \left[2P_{1,i}|h_{1,i}|^2 (1 + 2\rho P_{1,i}|h_{1,i}|^2)^{\frac{\beta_{1,i}}{M}-1} \right]}{\mathbb{E} \left[(1 + 2\rho P_{1,i}|h_{1,i}|^2)^{\frac{\beta_{1,i}}{M}} \right]} + \frac{1}{M \ln 2} \frac{\mathbb{E} \left[2P_{2,i}|h_{2,i}|^2 (1 + 2\rho P_{2,i}|h_{2,i}|^2)^{\frac{\beta_{2,i}}{M}-1} \right]}{\mathbb{E} \left[(1 + 2\rho P_{2,i}|h_{2,i}|^2)^{\frac{\beta_{2,i}}{M}} \right]} \right). \end{aligned} \quad (55)$$

Then we have that, $\lim_{\rho \rightarrow 0} \left(\frac{\partial \widetilde{E}_c^{tot}}{\partial \rho} \right) = \sum_{i=1}^{\frac{M}{2}} \left(\frac{2P_{1,i}}{M \ln 2} \mathbb{E}[|h_{1,i}|^2] + \frac{2P_{2,i}}{M \ln 2} \mathbb{E}[|h_{2,i}|^2] \right)$, and $\lim_{\rho \rightarrow \infty} \left(\frac{\partial \widetilde{E}_c^{tot}}{\partial \rho} \right) = \lim_{\rho \rightarrow \infty} \left(\sum_{i=1}^{\frac{M}{2}} \frac{1}{\rho M \ln 2} + \frac{1}{\rho M \ln 2} \right) = 0$.

So that, $\lim_{\rho \rightarrow 0} \left(\frac{\partial (E_c^{tot} - \widetilde{E}_c^{tot})}{\partial \rho} \right) = 0$.

By following similar approach, we also get, $\lim_{\rho \rightarrow \infty} \left(\frac{\partial (E_c^{tot} - \widetilde{E}_c^{tot})}{\partial \rho} \right) = 0$.

REFERENCES

- [1] S. R. Islam, N. Avazov, O. A. Dobre, and K.-S. Kwak, "Power-domain non-orthogonal multiple access (NOMA) in 5G systems: Potentials and challenges," *IEEE Commun. Surveys Tuts.*, vol. 19, no. 2, pp. 721–742, 2016.
- [2] B. Makki, K. Chitti, A. Behravan, and M.-S. Alouini, "A survey of noma: Current status and open research challenges," *IEEE Open J. Commun. Soc.*, vol. 1, pp. 179–189, 2020.
- [3] Z. Ding, X. Lei, G. K. Karagiannidis, R. Schober, J. Yuan, and V. K. Bhargava, "A survey on non-orthogonal multiple access for 5G networks: Research challenges and future trends," *IEEE J. Sel. Areas Commun.*, vol. 35, no. 10, pp. 2181–2195, 2017.
- [4] Y. Saito, A. Benjebbour, Y. Kishiyama, and T. Nakamura, "System-level performance evaluation of downlink non-orthogonal multiple access (noma)," in *IEEE 24th Annu. Int. Symp. Pers., Indoor, Mobile Radio Commun. (PIMRC)*, 2013, pp. 611–615.
- [5] Z. Ding, Z. Yang, P. Fan, and H. V. Poor, "On the performance of non-orthogonal multiple access in 5G systems with randomly deployed users," *IEEE Signal Process. Lett.*, vol. 21, no. 12, pp. 1501–1505, 2014.
- [6] Y. Saito, Y. Kishiyama, A. Benjebbour, T. Nakamura, A. Li, and K. Higuchi, "Non-orthogonal multiple access (NOMA) for cellular future radio access," in *Proc. IEEE Veh. Technol. Conf. Spring*, 2013, pp. 1–5.
- [7] K. Higuchi and A. Benjebbour, "Non-orthogonal multiple access (NOMA) with successive interference cancellation for future radio access," *IEICE Trans. Commun.*, vol. 98, no. 3, pp. 403–414, 2015.
- [8] J. He, Z. Tang, Z. Ding, and D. Wu, "Successive interference cancellation and fractional frequency reuse for LTE uplink communications," *IEEE Trans. Veh. Technol.*, vol. 67, no. 11, pp. 10528–10542, 2018.
- [9] N. I. Miridakis and D. D. Vergados, "A survey on the successive interference cancellation performance for single-antenna and multiple-antenna OFDM systems," *IEEE Commun. Surveys Tuts.*, vol. 15, no. 1, pp. 312–335, 2013.

- [10] T. Manglayev, R. C. Kizilirmak, Y. H. Kho, N. Bazhayev, and I. Lebedev, "NOMA with imperfect SIC implementation," in *IEEE EUROCON-17th Int. Conf. Smart Technol.*, 2017, pp. 22–25.
- [11] M. Chen and A. Burr, "Multiuser detection for uplink non-orthogonal multiple access system," *IET Commun.*, vol. 13, no. 19, pp. 3222–3228, 2019.
- [12] Y. Cai, Z. Qin, F. Cui, G. Y. Li, and J. A. McCann, "Modulation and multiple access for 5G networks," *IEEE Commun. Surveys Tuts.*, vol. 20, no. 1, pp. 629–646, 2018.
- [13] W. Shin, M. Vaezi, B. Lee, D. J. Love, J. Lee, and H. V. Poor, "Non-orthogonal multiple access in multi-cell networks: Theory, performance, and practical challenges," *IEEE Commun. Mag.*, vol. 55, no. 10, pp. 176–183, 2017.
- [14] S. M. R. Islam, M. Zeng, O. A. Dobre, and K. Kwak, "Resource allocation for downlink NOMA systems: Key techniques and open issues," *IEEE Trans. Wireless Commun.*, vol. 25, no. 2, pp. 40–47, 2018.
- [15] Q. Sun, S. Han, C. I, and Z. Pan, "On the ergodic capacity of MIMO NOMA systems," *IEEE Wireless Commun. Lett.*, vol. 4, no. 4, pp. 405–408, 2015.
- [16] M. Zeng, A. Yadav, O. A. Dobre, G. I. Tsiropoulos, and H. V. Poor, "Capacity comparison between MIMO-NOMA and mimo-oma with multiple users in a cluster," *IEEE J. Sel. Areas Commun.*, vol. 35, no. 10, pp. 2413–2424, 2017.
- [17] L. Zhu, J. Zhang, Z. Xiao, X. Cao, and D. O. Wu, "Optimal user pairing for downlink non-orthogonal multiple access (noma)," *IEEE Wireless Commun. Lett.*, vol. 8, no. 2, pp. 328–331, 2019.
- [18] F. Kara, F. Gemici, H. Hökelek, and H. A. Çirpan, "Optimal power allocation for dl noma systems," in *25th Signal Process. Commun. Appl. Conf.*, 2017, pp. 1–4.
- [19] N. Gleis and R. Belgacem Chibani, "Power allocation for energy-efficient downlink noma systems," in *2019 19th Int. Conf. Sci. Techn. Automat. Contr. Comput. Eng.*, 2019, pp. 611–613.
- [20] X. Diao, J. Zheng, Y. Wu, and Y. Cai, "Joint computing resource, power, and channel allocations for d2d-assisted and noma-based mobile edge computing," *IEEE Access*, vol. 7, pp. 9243–9257, 2019.
- [21] S. Xie, "Power allocation scheme for downlink and uplink noma networks," *IET Commun.*, vol. 13, no. 15, pp. 2336–2343, 2019.
- [22] K. Huang, Z. Wang, H. Zhang, Z. Fan, X. Wan, and Y. Xu, "Energy efficient resource allocation algorithm in multi-carrier noma systems," in *2019 IEEE 20th Int. Conf. High Perform. Switching and Routing (HPSR)*, 2019, pp. 1–5.
- [23] J. Tang, J. Luo, M. Liu, D. K. C. So, E. Alsusa, G. Chen, K. Wong, and J. A. Chambers, "Energy efficiency optimization for noma with swipt," *IEEE J. Sel. Topics Signal Process.*, vol. 13, no. 3, pp. 452–466, 2019.
- [24] M. Alkhatwahrah, Y. Gong, G. Chen, S. Lambotharan, and J. A. Chambers, "Buffer-aided relay selection for cooperative noma in the internet of things," *IEEE Internet Things J.*, vol. 6, no. 3, pp. 5722–5731, 2019.
- [25] P. Xu, J. Quan, Z. Yang, G. Chen, and Z. Ding, "Performance analysis of buffer-aided hybrid noma/oma in cooperative uplink system," *IEEE Access*, vol. 7, pp. 168 759–168 773, 2019.
- [26] M. Pischella, A. Chorti, and I. Fijalkow, "Performance analysis of uplink noma-relevant strategy under statistical delay qos constraints," *IEEE Commun. Lett.*, vol. 9, no. 8, pp. 1323–1326, 2020.
- [27] W. Yu, A. Chorti, L. Musavian, H. Vincent Poor, and Q. Ni, "Effective secrecy rate for a downlink NOMA network," *IEEE Trans. Wireless Commun.*, vol. 18, no. 12, pp. 5673–5690, 2019.
- [28] A. Chorti and H. V. Poor, "Achievable secrecy rates in physical layer secure systems with a helping interferer," in *2012 Int. Conf. Comput., Netw. Commun. (ICNC)*, 2012, pp. 18–22.
- [29] W. Yu, L. Musavian, and Q. Ni, "Tradeoff analysis and joint optimization of link-layer energy efficiency and effective capacity toward green communications," *IEEE Trans. Wireless Commun.*, vol. 15, no. 5, pp. 3339–3353, 2016.
- [30] D. Wu and R. Negi, "Effective capacity: a wireless link model for support of quality of service," *IEEE Trans. Wireless Commun.*, vol. 2, no. 4, pp. 630–643, 2003.
- [31] J. Tang and X. Zhang, "Cross-layer modeling for quality of service guarantees over wireless links," *IEEE Trans. Wireless Commun.*, vol. 6, no. 12, pp. 4504–4512, 2007.
- [32] L. Musavian and Q. Ni, "Effective capacity maximization with statistical delay and effective energy efficiency requirements," *IEEE Trans. Wireless Commun.*, vol. 14, no. 7, pp. 3824–3835, 2015.
- [33] W. Yu, L. Musavian, and Q. Ni, "Link-layer capacity of NOMA under statistical delay QoS guarantees," *IEEE Trans. Commun.*, vol. 66, no. 10, pp. 4907–4922, 2018.

- [34] M. Bello, W. Yu, A. Chorti, and L. Musavian, "Performance analysis of noma uplink networks under statistical qos delay constraints," in *ICC 2020 - 2020 IEEE Int. Conf. Commun. (ICC)*, 2020, pp. 1–7.
- [35] M. B. Shahab, M. Irfan, M. F. Kader, and S. Shin, "User pairing schemes for capacity maximization in non-orthogonal multiple access systems," *Wireless Commun. Mobile Comput.*, vol. 16, pp. 2884–2894, 09 2016.
- [36] E. Biglieri, G. Caire, and G. Taricco, "Limiting performance of block-fading channels with multiple antennas," *IEEE Trans. Inf. Theory*, vol. 47, no. 4, pp. 1273–1289, 2001.
- [37] Z. Yang, Z. Ding, P. Fan, and N. Al-Dhahir, "A general power allocation scheme to guarantee quality of service in downlink and uplink NOMA systems," *IEEE Trans. Wireless Commun.*, vol. 15, no. 11, pp. 7244–7257, 2016.
- [38] N. Zhang, J. Wang, G. Kang, and Y. Liu, "Uplink nonorthogonal multiple access in 5G systems," *IEEE Commun. L.*, vol. 20, no. 3, pp. 458–461, 2016.
- [39] L. Fan, S. Jin, C.-K. Wen, and H. Zhang, "Uplink achievable rate for massive MIMO systems with low-resolution ADC," *IEEE Commun. L.*, vol. 19, no. 12, pp. 2186–2189, 2015.
- [40] H.-C. Yang and M.-S. Alouini, *Order statistics in wireless communications: diversity, adaptation, and scheduling in MIMO and OFDM systems*. Cambridge University Press, 2011.
- [41] H. Sun, B. Xie, R. Q. Hu, and G. Wu, "Non-orthogonal multiple access with sic error propagation in downlink wireless mimo networks," in *2016 IEEE 84th Veh. Technol. Conf.*, 2016, pp. 1–5.